

# POLITECNICO DI TORINO

Master of Science in Energy and Nuclear Engineering



Master of Science Thesis

Drones in photovoltaic fields maintenance

Tutor

prof. Filippo Spertino

Student

Silvia Nitti

Academic year 2018/2019



A mamma e papà,  
costantemente dalla mia parte

## **Abstract**

The present study has been developed at Enel Green Power, Italian company leader in the energy sector, in particular within the Technical Support of the Solar Competence Center in Operation & Maintenance.

In a long project of robotization that the company is carrying out, drones have a fundamental role: it has been analysed how to employ them during PV field maintenance and when it is cost effective, according to plant capacity. The main use of drones is associated to thermography and visual inspection, so it has been carried out a deepening on these methods of maintenance and on the modules faults that they can find, considering only polycrystalline silicon technology.

Later, based on field experience, the technical specifications for the survey have been drawn up, also giving indications on the purchase of the appropriate hardware (drone and camera) to the various Countries in which EGP has its PV plants.

Then, considering the thermographic reports of six photovoltaic fields, the failure rate of modules has been estimated and a categorization of the failures affecting the panels has been done. At this point the energy assessment has been carried out, as a result of which it has been possible to estimate the losses associated with the abovementioned faults.

Finally, an economic analysis has been performed. Considering capital expenditure, operational expenditure and incomes, a model has been created. The Net Present Value of the investment has been calculated to establish when it is economically viable to buy a drone, based on installed MW.

# Table of Contents

1	Introduction.....	7
1.1	Global Situation .....	7
2	Structure of the photovoltaic system.....	12
2.1	Main components .....	14
2.2	Auxiliary Systems .....	21
3	Operation & Maintenance .....	23
3.1	I-V curve.....	24
3.2	Electroluminescence.....	26
3.3	Visual inspection.....	27
3.3.1	Visual inspection in laboratory.....	28
3.3.2	Visual inspection in the field.....	28
3.4	Thermography.....	28
3.4.1	Pulse thermography .....	29
3.4.2	Lock-in thermography .....	29
3.4.3	Thermography under steady state conditions.....	30
3.5	Robotization in O&M.....	30
3.5.1	Exoskeleton .....	30
3.5.2	Smart glasses .....	31
3.5.3	Cleaning machine .....	31
3.5.4	Grass cutting machine.....	33
3.5.5	Drones .....	34
4	Polycrystalline modules failures .....	37
4.1	Polycrystalline module .....	37
4.2	Definition of failure.....	39
4.2.1	Physical anomalies .....	41

4.2.1.1	Shattering.....	41
4.2.1.2	Soiling .....	42
4.2.1.3	Snail tracks .....	43
4.2.1.4	Burn marks .....	44
4.2.1.5	Delamination .....	45
4.2.2	Thermal anomalies .....	46
4.2.2.1	Electrical mismatch.....	46
4.2.2.2	Shadowing and activated bypass diode.....	47
4.2.2.3	Potential Induced Degradation (PID).....	48
4.2.2.4	Encapsulant discolouration.....	49
5	Guidelines for the use of drones in the field.....	51
5.1	Countries management .....	51
5.2	Choice of drone .....	52
5.3	Choice of camera.....	55
5.4	Raptor Maps.....	57
5.5	Technical Specifications .....	60
5.5.1	Brief resume of the requirements of the thermal sensor .....	60
5.5.2	Recommended annual inspection intervals .....	61
5.5.3	Flight directives .....	61
5.5.4	Additional documentation.....	66
5.5.5	Inspection time and delivery guidance .....	66
6	Faults found in the field.....	67
6.1	Thermographic reports .....	67
6.1.1	Plant 1: Rubi.....	67
6.1.2	Plant 2: Villanueva .....	68
6.1.3	Plant 3: Dodge Center.....	68
6.1.4	Plant 4: Woods Hill .....	69
6.1.5	Plant 5: Atwater.....	70
6.1.6	Plant 6: Paynesville.....	71

6.2	Failures categorization.....	71
6.3	Energy assessment.....	76
6.4	Energy losses.....	77
7	Economic Analysis.....	80
7.1	Net Present Value methodology.....	80
7.2	Application.....	82
7.2.1	Capex .....	82
7.2.2	Opex.....	83
7.2.3	Incomes .....	84
7.3	Conclusions.....	86
8	Future evolutions.....	90

## List of figures

Figure 1.1 Photovoltaic growth by Country in 2017 .....	8
Figure 1.2 Global renewable power capacity growth from 2007 to 2017.....	8
Figure 1.3 Global photovoltaic power capacity growth from 2007 to 2017 .....	9
Figure 1.4 Forecasts on the global development of photovoltaics .....	11
Figure 2.1 Standard pattern of PV plant.....	13
Figure 2.2 Photovoltaic connectors.....	14
Figure 2.3 Fuses DC side .....	16
Figure 2.4 DC switches equipped with rotary knobs .....	17
Figure 2.5 Scheme of PV plant: strings, string boxes, parallel boxes and inverter .....	18
Figure 2.6 Inverter.....	19
Figure 2.7 MPPT operation .....	20
Figure 3.1 Example of I-V curve for an illuminated module .....	24
Figure 3.2Irradiance effect on I-V curves .....	25
Figure 3.3 Temperature effect on I-V curves .....	26
Figure 3.4 Cell crack detected by electroluminescence .....	27
Figure 3.5 Plausible application scenario of the exoskeleton.....	31
Figure 3.6Plausible application scenario of the smart glasses.....	31
Figure 3.7 Example of cleaning machine .....	32
Figure 3.8 Example of grass cutting machine .....	33
Figure 3.9 Drone flying over a PV field.....	34
Figure 3.10 Automated thermography process.....	36
Figure 4.1 PV module with 72 solar cells in series.....	37
Figure 4.2 Module price over the years.....	39
Figure 4.3 Example of shattering .....	41
Figure 4.4 Example of soiling .....	42
Figure 4.5 Example of snail track .....	43
Figure 4.6 Example of burn marks .....	44
Figure 4.7 Examples of delamination .....	45
Figure 4.8 Example of electrical mismatch .....	47
Figure 4.9 Example of shadowing .....	47

Figure 4.10 activated bypass diode through thermography .....	48
Figure 4.11 Example of PID.....	49
Figure 4.12 Example of EVA discolouration .....	50
Figure 5.1 Drone during a wind turbine inspection .....	52
Figure 5.2 FoV comparison .....	57
Figure 5.3 Difference among lenses .....	60
Figure 5.4 GSD for the three levels .....	61
Figure 5.5 Flight path.....	62
Figure 5.6 Gimbal pitch.....	62
Figure 5.7 Typical flight parameters.....	63
Figure 5.8 Sensor orientation.....	63
Figure 5.9 DJI Ground Station Pro Settings for Level II flight .....	64
Figure 5.10 Example of oblique image of PV plant .....	65
Figure 6.1 Rubi findings.....	67
Figure 6.2 Villanueva findings .....	68
Figure 6.3 Dodge Center findings.....	69
Figure 6.4 East Woods Hill findings.....	69
Figure 6.5 West Woods Hill findings .....	70
Figure 6.6 Atwater findings.....	70
Figure 6.7 Paynesville findings .....	71
Figure 6.8 Percentage of individual error categories .....	75
Figure 6.9 Bathtub curve .....	78
Figure 6.10 Module failure rate in 25 years .....	79
Figure 7.1 Forecasts on module price .....	84
Figure 7.2 NPV at 25 years for plants with different size .....	86
Figure 7.3 Cumulative cash flow for 30 MW plant .....	87
Figure 7.4 Cumulative cash flow for 50 MW plant .....	88
Figure 7.5 Cumulative cash flow for 500 MW plant.....	88
Figure 8.1 Photo of the first Percepto flight in Totana, Spain.....	90

## List of tables

Table 4.1 Different PV cell technologies .....	37
Table 4.2 Power loss category .....	40
Table 5.1 Useful drones for each Country .....	52
Table 5.2 Drones selection .....	54
Table 5.3 Cameras selection .....	56
Table 5.4 Annual inspections intervals .....	61
Table 6.1 Resume of thermographic reports .....	73
Table 6.2 Description of anomalies .....	74
Table 6.3 Energy losses associated to fault category .....	75
Table 6.4 Equivalent operating hours for each PV plant .....	77
Table 7.1 Component for WACC calculation .....	81
Table 7.2 Capex .....	82
Table 7.3 Costs and incomes .....	86
Table 7.4 Pay Back Time .....	89

# 1 Introduction

Global energy demand has increased proportionally to demographic growth and improvement of economic situation in many Countries. While energy demand is increasing, its primary sources, i. e. fossil fuels, are steadily decreasing because of the excessive consumption and of their limited availability.

In the last years we all are living the consequences of this over-consumption: global warming, melting of the glaciers at the north and south poles, damage to the ozone layer are the most important marks of the climate change.

Renewable energy sources are the principal solution to this dire situation, only decreasing fossil utilization and creating less waste, we can try to avoid further environmental damages. Solar energy exploitation, in particular through photovoltaic technology (PV), has an important role in this panorama. Many countries are planning the intensification of electricity from alternative sources compared to traditional ones, consequently photovoltaic power plants are increasing all over the world.

Photovoltaics has aroused great interest from researchers, producers and decision makers as a source of clean energy generation due to its economic and environmental benefits. There is great potential for the use of high efficiency photovoltaic systems in different areas of the world due to the high amount of solar radiation incident in these regions. Photovoltaics is one of the most developed renewable technologies, thanks to its numerous and promising advantages, such as the lack of complex maintenance and low operating costs, long service life and reduction of CO<sub>2</sub> emissions, features which lead to the achievement of important results, such as mainly a despite population growth and increased energy consumption.

## 1.1 Global Situation

During 2017, the world added more capacity from solar PV than from any other type of power generating technology, it was a milestone year. Worldwide, at least

98 GW<sub>dc</sub> of solar PV capacity was installed, increasing total capacity by approximately one-third, for a total value of 402 GW.

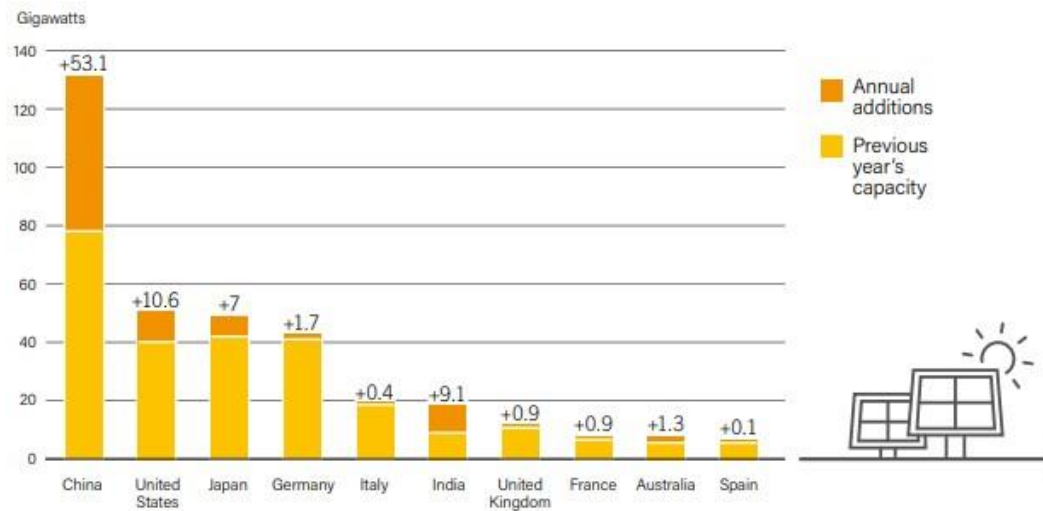


Figure 1.1 Photovoltaic growth by Country in 2017

This fully reflects the growth of renewable power with an installed capacity of about 178 GW worldwide. Compared to 2016 there was a growth of 9%, of which 55% concerns the photovoltaic sector itself.

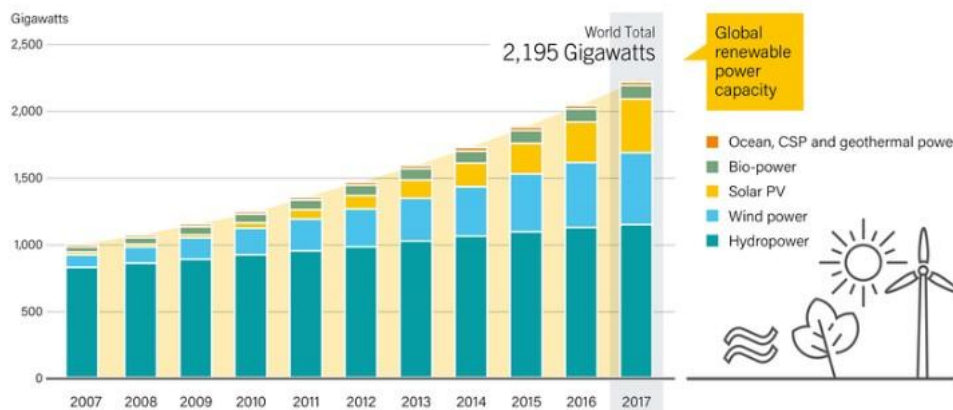
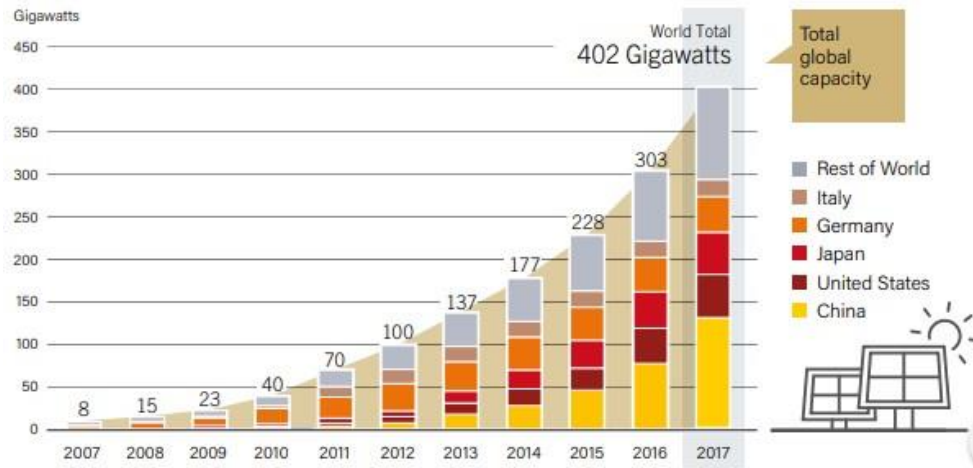


Figure 1.2 Global renewable power capacity growth from 2007 to 2017

The news of the last years is that new markets are emerging. Countries on all continents have begun to contribute to global growth, thanks to incentives and regulations driven by government, even if the biggest concentration is still in a minority of “old” Countries.



*Figure 1.3 Global photovoltaic power capacity growth from 2007 to 2017*

In fact, when solar photovoltaic systems have been recognized as promising renewable energy technologies, several governments implemented political and economic programs with the aim of providing economic incentives for investment. For many years, mainly Japan and cutting-edge European countries have driven growth and as a result, thanks to technological improvements and economies of scale, the cost of solar energy has decreased significantly. This trend does not seem to stop, to the point that photovoltaics is expected to become the world's largest source of electricity by 2050: to reach this aim installed capacity should grow up until 4.600 GW.

Over the past decades, many nations' governments have met at various conferences, reaching agreements and signing protocols with the aim of limiting human environmental impact and taking paths towards energy and environmental sustainability.

The 21<sup>th</sup> session of Conference of Parties (COP 21) at United Nation Framework Convention on Climate Change (UNFCCC) in Paris, in December 2015, is finished with a fundamental pact to keep global warming as close to 1,5°C as possible. There was general agreement that the nationally determined contributions (NDC) proposed by each country were only a first step towards achieving the objectives of the Paris Agreement. In a recent publication Sir Robert Watson, former president of the Intergovernmental Panel on Climate Change (IPCC), and co-authors said that global greenhouse gas emissions (GHG) should not decrease fast enough to stay

below 2°C. According to this analysis, 1.5°C would be reached by 2030 and the target of 2.0°C by 2050.

Decarbonisation of our energy supply is a key component in achieving the targets, as 65% of the world's current CO<sub>2</sub> emissions are due to the use of fossil fuels. In 2014, 81% of our total primary energy supply depended on the combustion of hydrocarbons, i.e. 29% coal, 31% oil and 21% natural gas. In terms of final energy consumption, electricity accounted for only 18.1%, but was responsible for 35.2% of total CO<sub>2</sub> emissions. Photovoltaics (PV) and wind power are key technological options for moving to a decarbonized energy supply and can be distributed in a modular way almost anywhere on the planet. To realise a carbon free power supply by 2050, the installed PV generation capacity of about 500 GW at the end of 2018 has to increase to more than 4 TW by 2025 and 21.9 TW by 2050 to make it happen. The European Union needs to increase its capacity from 115 GW at the end of 2018 to more than 631 GW by 2025 and 1.94 TW by 2050. In case of a transition to a sustainable transport sector, i.e. electrification and synthetic fuels, these numbers would increase by a factor of two.

Despite the significant growth in the use of non-hydro renewable energy over the last decade, there are structural obstacles to the use of all renewable energy sources. Especially in the electricity sector, the current design of the European system, both economically and politically and socially, still favours the centralised use of conventional energy (coal, oil, natural gas and nuclear energy), this situation therefore results in a high cost from the point of view of economic vision for making an energy transition to a sustainable energy supply. In addition, the current electricity distribution system was designed for unidirectional flow from centralized units to consumers, while decentralised generation of renewable solar and wind energy requires the capacity of a two-way flow of electricity.

In the European Union, conditions for photovoltaics market vary considerably from one country to another due to the existent different energy policies. Between 2005 and 2015, the EU's photovoltaic solar power generation capacity has shifted from 1,9 GW to 95,4 GW. Already in 2014, the NREAP target (National Action Plan for renewable energy 2020) of 83.7 GW was exceeded, reaching about 88.4 GW. With

a total installed capacity of 95.4 GW at the end of 2015, the EU still accounted for 40.6% of the global 235 GW of photovoltaic solar power generation capacity, although this was lower than the 66% recorded at the end of 2012.

According to the 2016 report of the medium-term renewable energy market of the IEA, the share of installed solar capacity in the EU will fall below 30% by 2020 due to a stagnant market of 7-8 GW. Support schemes in some Member States have not been designed to react quickly enough to the fast moving market growth, and as a result, these markets have developed unsustainable growth rates and the governments have reacted with sudden and unpredictable changes in support schemes, as well as legal requirements. This resulted in installation peaks before deadlines and high uncertainty for potential investors. In addition, a number of retroactive measures have further reduced investor confidence.

*Renewables 2018*, the International Energy Agency review, has underlined the presence of other international subjects. In the next five years, other RES technology should follow blindly PV one, thanks to the important investments made in Pacific Asia area, in particular in China.

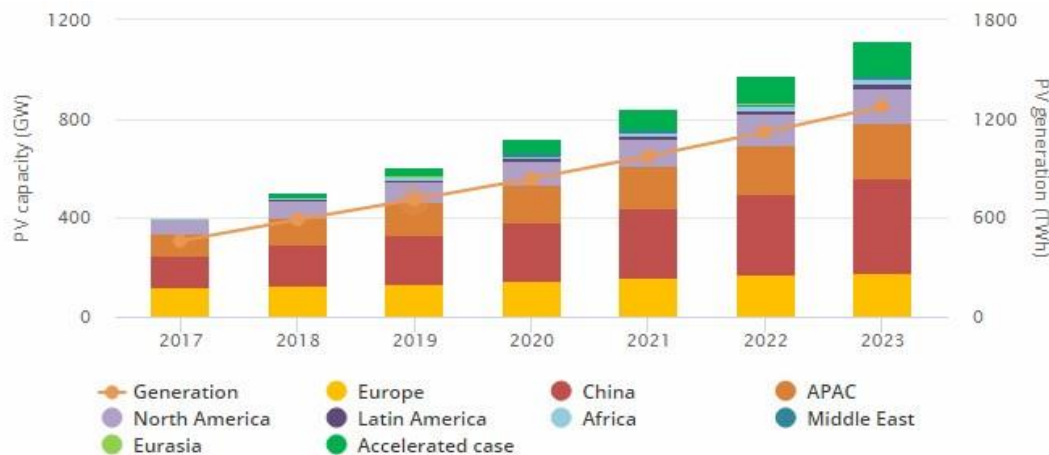


*Figure 1.4 Forecasts on the global development of photovoltaics*

The graph shows how much the presence of these emergent world powers affects the photovoltaics growth: evidently, the old leaders in the field give way to new players in the energetic sector.

## 2 Structure of the photovoltaic system

Designing a megawatt-scale solar PV power plant is a process that requires technical knowledge and experience. Despite the fact that it is a well-known and well-established technology, the solar system is composed of several components that can cause a series of technical issues; hence it is important to strike a balance between cost savings and quality.

The performances of a solar PV power plant can be optimised by reducing the system losses, whose presence is due to components quality, too.

We must remember that there are three many applications of photovoltaic systems:

- Residential plants connected to low voltage;
- Production plants connected to middle or high voltage;
- Plants with storage systems (i.e. batteries) for off-grid users. In this study, the second category has been deepened, since EGP owns big production plants in different Countries of the world.

There are many variables that distinguish a photovoltaic plant from another one (power, dimension, geometry, technology, climate etc...) determining the uniqueness of each of them. For this reason, it cannot exist a unique scheme that represents every PV plant, but we can give a standard pattern in which the main (and necessary) components are included.

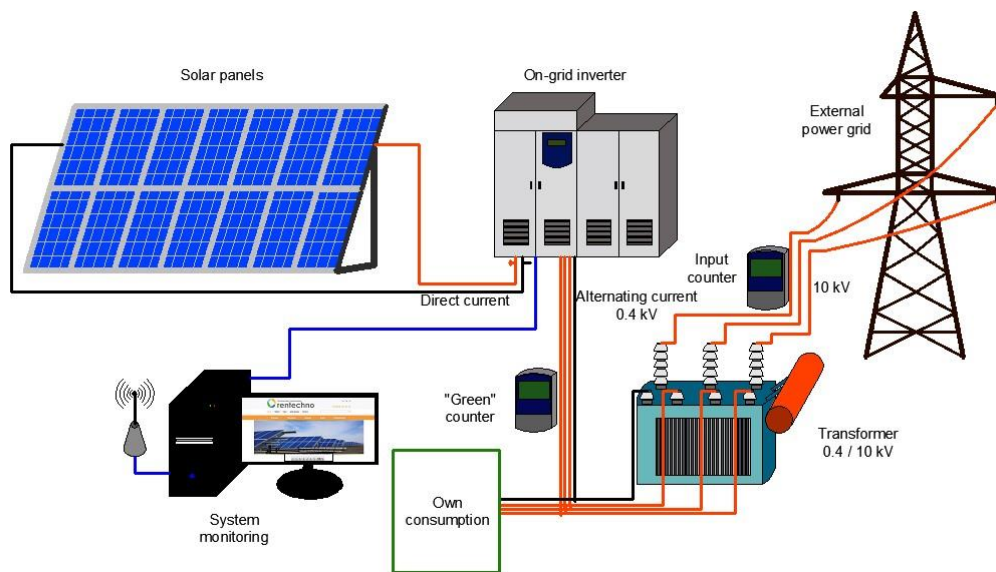


*Figure 2.1 Standard pattern of PV plant*

The policy implemented in recent years by Enel Green Power is to build medium-large photovoltaic plants, expanding in new territories to increase its production of clean energy. All the plants analysed have less than 1 year of life, so they have a similar layout.

The typical components of a photovoltaic field are:

- PV generator;
- String box;
- Conversion unit;
- Substation HV (connection to the grid).

Then there also auxiliary systems

- Auxiliary systems feeder;
- LV switchboard;
- UPS;
- Data transfer system;
- SCADA;

- CCTV (closed-circuit television): a system of remote monitoring using cameras;
- Fire detection system;
- Field sensors associated to a meteo station.

## 2.1 Main components

The first element to analyse in a photovoltaic field is surely the module. The most diffused model is the one composed by polycrystalline silicon cells and EGP tends to use this kind of technology, too. A better description has been developed in the chapter 4.

Photovoltaic connectors are elements with a copper core and made of plastic outside whose aim is to connect PV modules in series. They are sold in pairs (a male and a female), and when linked, they are theoretically resistant to bad weather and waterproof. Actually, connectors are often subject to failures due to their oxidation.



*Figure 2.2 Photovoltaic connectors*

Panels are usually disposed in string made of 30 modules. In every plants there are tracker structures, they can control 2 or 3 strings. This depends on territory topography, trying to make the best use possible of the spaces.

Beyond the strings, there is the string-box, it is a device that connects in parallel strings of PV modules for connection to the inverter. Its functions are:

- to allow a number of strings to be connected in parallel;
- to allow the isolation of any defective strings;

- to protect the inverter from possible input overvoltages;
- to facilitate maintenance operations on the direct current section of the system;
- to allow the acquisition of measures for monitoring the photovoltaic field (string currents, sensors): this only if it is a smart string box;
- to allow the disconnection under load of the entire group of strings afferent to the switchboard.

This component is principally constituted by three elements: fuses, block diodes and DC switch. The fuses shown in figure 2.3 behave like circuit breakers, as they contain a filament that remains intact if it does not reach a certain temperature. If, on the other hand, through the fuse a current higher than that for which it was designed passes, the fuse overheats and melts interrupting the circuit, then it must be replaced. The photovoltaic modules generate direct current through solar radiation, the current is sent to an inverter that transforms it into alternating current. The fuses in the DC section of the photovoltaic system provide overcurrent protection by disconnecting the photovoltaic modules from the inverter. These fuses protect the panels from reverse overcurrent and the inverter from direct or indirect overcurrent caused, for example, by lightning. Fuses are always applied to both the positive and negative poles of the DC circuit. Fast type fuses designed for use in photovoltaics, with low minimum current, are used. When three or more strings are connected in parallel, as in all the cases analysed in this study, a fuse on each string will protect the cables from damage and help minimize safety risks. It will isolate the damaged string so that the rest of the PV system can continue to produce electricity. There are a few design rules for the size of fuses. The maximum current in a string circuit will be about 125% of the panel short-circuit current ( $I_{sc}$ ). The cables and overcurrent protection devices must therefore be sized at 125% of the maximum circuit current. In addition, international standards such as EN7671 Sect. 712 for systems powered by photovoltaic panels stipulate that the cables of such systems must be sized to conduct a current greater than or equal to  $1.25 \times I_{sc}$ , where this one is measured at standard conditions, i.e. STC (Standard Test

Conditions: radiation of  $1,000 \text{ W/m}^2$  and cell temperature  $25^\circ\text{C}$ ). The manufacturers of photovoltaic modules report the value of  $I_{sc}$  on their datasheets.



*Figure 2.3 Fuses DC side*

Blocking diodes are used to isolate one or more strings from each other and to ensure that, as a result of a short circuit or shading, the other strings continue to generate and that there is no current reversal in the inactive string. The blocking voltage of the diode must be greater than the open-circuit voltage of the string in STC. The passage of current within the string diode usually results in losses of the order of  $0.5\% \div 2\%$  caused by a voltage drop in the crossing of about  $0.5 \div 1 \text{ [V]}$ , such as losses are acceptable when compared to the benefits that the same component brings to the system.

The DC switch, shown in figure 2.4, is an important part of the photovoltaic system safety, whose reliability and stability refer to the stable generation of energy. Grid safety is a fundamental factor in the operation of a photovoltaic system that generates a stable energy. Photovoltaic modules must be able to be disconnected from the system at the power supply point in the event of a fault. It is also necessary to avoid grid supply in the event of mains and system faults. The standards require the disconnects to be located on both sides of the inverter, these must be characterized by a load switching capacity suitable on both sides DC and AC. As the PV connection system generally cannot be disconnected under load such as for maintenance work, it is absolutely necessary that switch-off equipment is supplied. The DC isolator is often already integrated in the inverter. However, these DC

switches are often also recommended in string survey to allow for selective disconnection of one or more PV strings. This allows the rest of the system to continue to produce electricity.



*Figure 2.4 DC switches equipped with rotary knobs*

Between string boxes and inverters there are parallel switchboards that put various strings in parallel, this is connected to the inverter inside the conversion unit.

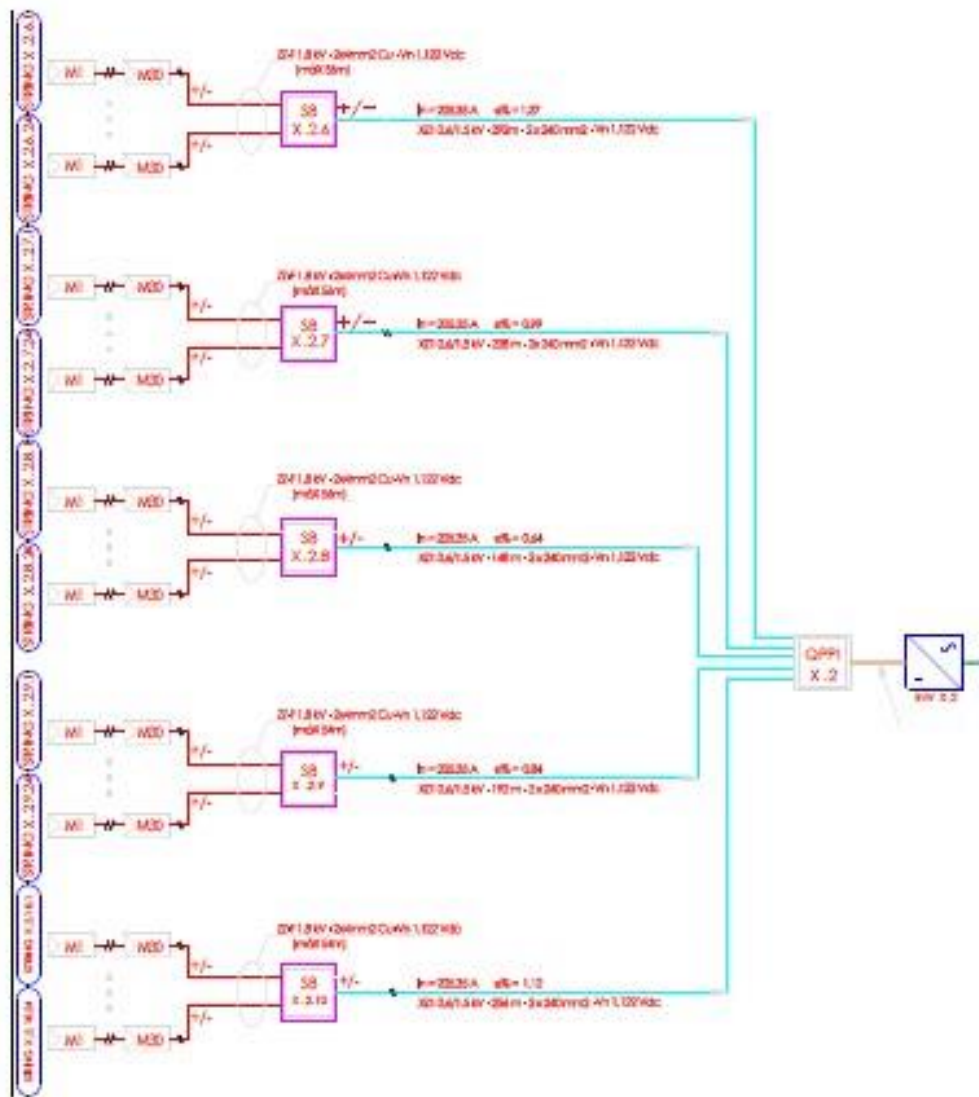


Figure 2.5 Scheme of PV plant: strings, string boxes, parallel boxes and inverter

The Conversion Unit is a set of electrical components that converts DC energy from a photovoltaic subfield in AC energy and transfers energy growing up the voltage level. A Conversion Unit has to:

- be a “plug and play system”;
- get electrical power of about 4 MVA;
- be compliance with local standard;
- include three separated rooms (for inverter, transformer and switchgear);

- level of protection  $\geq$  IP 33.

Inverter, ML/LV transformer, MV switchgear and auxiliary systems compose it.

The inverter is the heart of the photovoltaic system. The main purpose of the inverter is to transfer, on the alternating current side, in the most efficient way possible, the energy "delivered" to it in direct current, by the photovoltaic generator.

Therefore, if an appropriate "coupling" between the inverter and the "PV field" is not carried out, there is a risk that the system may run into frequent inefficiencies or fail to function at its best. The choice of its type and the philosophy adopted for the architecture of the system (number and arrangement of inverters), heavily depends on the functionality of the photovoltaic system and the quality of the installation.

The latest generation of large central inverters, available on the market in sizes of a few hundred kilowatts, are able to spatialize the machine on different modules, which give great flexibility and security to the system. In fact, in the event of failure of a module is still guaranteed the operation of the machine at partial load and you can extract the "drawer" of the module out of service to send it to technical assistance.

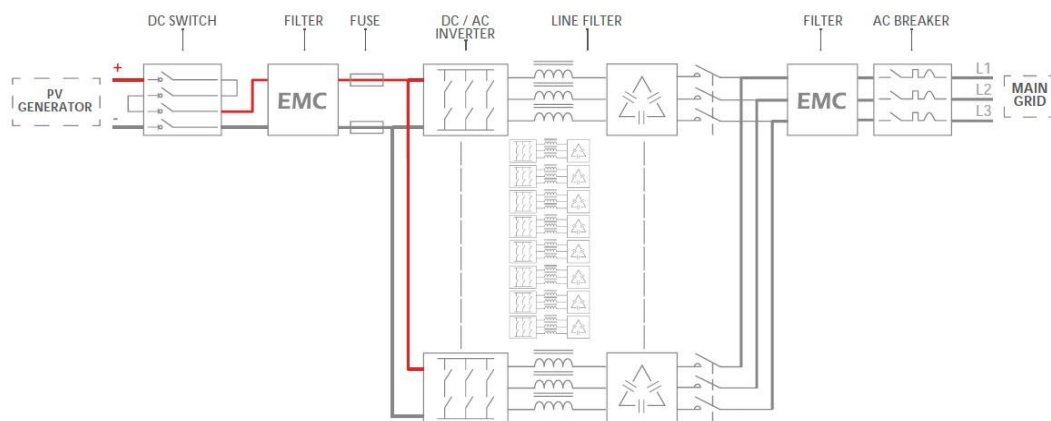


Figure 2.6 Inverter

One of its special functions is to function as a Max Power Point Tracker (MPPT). The task of the MPPT is to ensure the operation of the photovoltaic system, always at the point of maximum power, to vary the ambient conditions (radiation, temperature). In principle, the MPPT system is able to vary, within a certain range, the amount of load "seen" by the PV generator, operation is continuous, thus guaranteeing the most efficient functioning of the photovoltaic system at all times. Enel Green Power chooses this type of inverters that guarantee a system maximum voltage of 1500 V

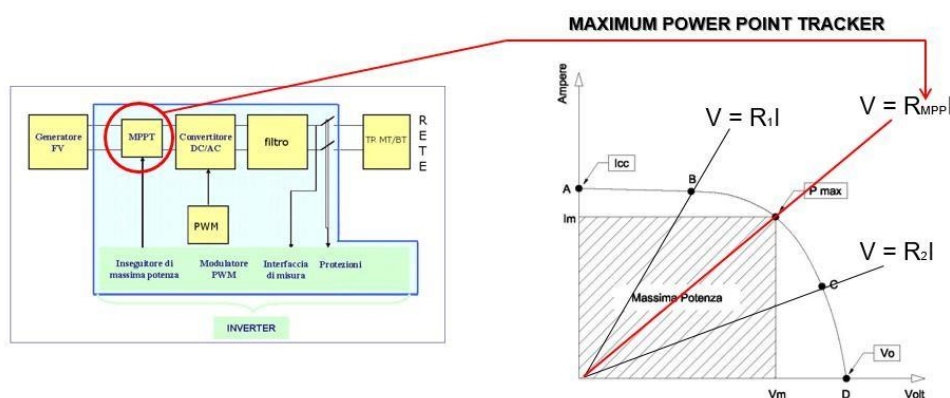


Figure 2.7 MPPT operation

In addition, a solar inverter has the task of monitoring the modules of the photovoltaic field and report problems and errors. At the same time, it must also monitor the grid it is connected to, so that if the photovoltaic generators or the grid have an issue, the system disconnects quickly and securely. Some inverters, now the most of them, are equipped with communication interfaces that allow the control and the monitoring of operational and production parameters.

Transformer is used to change (transform) the electrical parameters (voltage and current intensity) from a primary to a secondary network, keeping the apparent electrical power constant, and the switchgear is a protection for it and stops the feeding when necessary to work in safety.

Conversion unit output is energy at middle voltage, and then to increase the power, high voltage is needed, so the last step is a high voltage substation, which is directly connected to the grid.

A main switch for the system must be installed upstream of the network interface. This element is a switch, often motorized, placed immediately before the feed-in, which is coupled with a residual current device to protect the system in the event of a ground fault. This component, despite its simplicity, can interrupt the system, so that in the event of a system failure or of its entry into operation, can take on an important role in reducing production of energy in the system. It is essential to be well sized and checked periodically.

In medium and large size plants, two separate counters are usually inserted. The first counter is inserted upstream of the grid interface and downstream of the feeding of current into LV to the user. The purpose of this meter is to measure the energy actually generated by the plant. The second one is installed upstream of the main switch and downstream of the MV input. This device must be bidirectional in order to be able to count the energy fed into the grid and withdrawn from it.

## 2.2 Auxiliary Systems

After the main and indispensable components of the plant, let us analyse the auxiliary systems.

Among them, there is the SCADA, Supervisory Control And Data Acquisition. The SCADA system performs supervision, control and real time data acquisition of the PV plant; it is a software installed in a computer inside the conversion unit that takes data from inverter; from here, every information is shared with the central base and it is an essential component for Operation & Maintenance workers. There is also a plant SCADA that reads all values from CU SCADAs and from the various field sensors (an example is the pyranometers).

Each cabin includes a grounding and equipotential system built in copper, important for the safety in plant.

Meteo station is one in every plant and stores meteorological data, useful to understand if the plant is working well. An example of these data use is irradiance-power curves.

Every photovoltaic system that feeds energy into the grid must, as a rule, be equipped with a grid interface element. This component is not connected to the operation of the photovoltaic system, but has the function of managing the connection and optimal integration to the network. Renewable sources, as it is well known, are intermittent sources of energy, not totally predictable because create discontinuous and irregular energy inputs. The main purpose of the interface is to protect the grid from its own anomalies, thus interrupting the feed-in of electricity from the photovoltaic system, in case the grid is saturated with energy or in case of power failure or some parameters of the grid are off-axis. For plants with a peak power of more than 20 KW or with more than three inverters, therefore for all the systems analysed in the current study, the grid interface must be external to the inverter and must be installed separately.

### 3 Operation & Maintenance

Health monitoring and diagnosis of photovoltaic systems is crucial to maximise the power production, increase the reliability and life service of power plants. For this reason, many companies have a dedicated sector, Operation & Maintenance, whose aim is to keep the highest as possible the plant's level.

There are three different types of maintenance: preventive, predictive and corrective.

The preventive maintenance is carried out at predetermined intervals or according to prescribed criteria and is aimed at reducing the probability of failure or the degradation of the functioning of an item. It has the meaning of "prevent" the occurrence of the fault, in fact, if preventive action is carried out with effectiveness, the component replacing occurs when it is still functioning and therefore the fault is avoided. Moreover, it has the goal to comply with manufacturer guidelines, normative or legal requirements and obtain transparency about status of asset. Therefore, the preventive maintenance is proactive and strategically driven.

The predictive Maintenance activities include all controls made to monitor vibrations, heat, pressure, noise, thickness of the equipment and tries to identify the time remaining before the fault through mathematical models.

Solar power plants are subject to faults during operation that can require corrective maintenance activities whose aim is to put an item into a state in which it can perform a required function. The corrective maintenance includes three kind of maintenance activities: fault diagnosis (also called troubleshooting) to identify fault cause and localization, repair and temporary repairs.

Since the modules are the most important component of the PV system and their cost represents a high portion of the total investment, all large PV plant construction must incorporate a suitable quality control of photovoltaic modules to ensure the profitability of the project. This control begins with the introduction of the technical parameters of the quality control program and acceptance and rejection plan of batches in the supply contract, thus it permits to avoid possible conflicts between

manufacturer and client due to test results. It continues with on field operation whose aim is to monitor PV plant performance over the years.

Obviously, maintenance activities are numerous: some of them are set out below.

### 3.1 I-V curve

The relationship between the direct current (DC) flowing in an electronic device and the voltage measured at its terminals is the current-voltage characteristic, it is a graph in which I varies depending on V.

We can apply this graph to valuate solar cell performances. Every solar cell in c-Si, with rated irradiance, supplies voltage of  $0.5\div 0.6$  V (almost independent from the surface) and current (proportional to surface) with current density  $J_{sc}=25-35$  mA/cm<sup>2</sup>.

From the I-V curve, some key parameters can be extracted to access the quality of the cell; they are represented in figure 3.1, which shows a typical illuminated PV module curve (tested in laboratory).

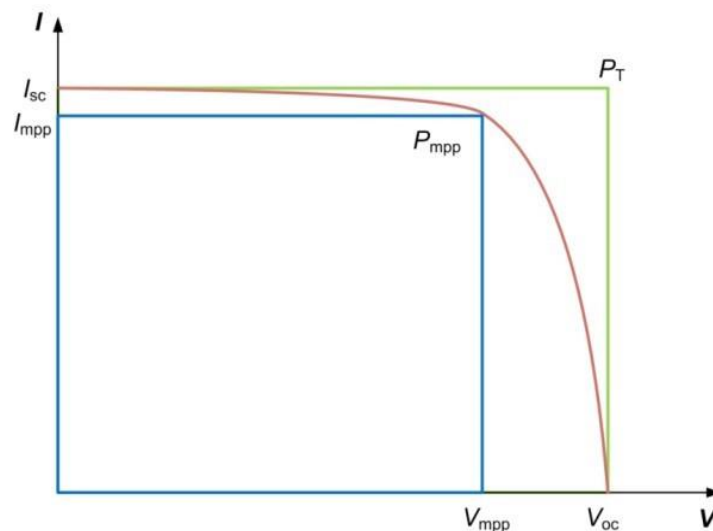


Figure 3.1 Example of I-V curve for an illuminated module

Let us analyse the quantities in the graph:

- Open-circuit voltage ( $V_{oc}$ ): extreme voltage obtainable from a PV cell that occurs at  $I=0$
- Short-circuit current ( $I_{sc}$ ): current flowing into the module when the  $V=0$
- Maximum power ( $P_{max}$ ): maximum power is the point where the product of current and voltage is maximum, hence at  $I_{mpp}$  and  $V_{mpp}$ .
- Virtual power ( $P_T$ ): power that would outcome if  $V_{mpp} = V_{oc}$  and  $I_{mpp} = I_{sc}$ . The ratio between  $P_{mpp}$  and  $P_T$  is the fill factor (FF) that is a measure of the cell quality; graphically it can be interpreted as the ratio of the rectangular areas of the figure 3.1. Typical values for c-Si are 0.7-0.8.

I-V curve of a solar cell changes for irradiance and temperature variations:

- Dependence on irradiation:  $I_{sc}$  and  $I_{mpp}$  change with the incident irradiance, and  $V_{oc}$  and  $V_{mpp}$  have minor variations (for the logarithmic law):

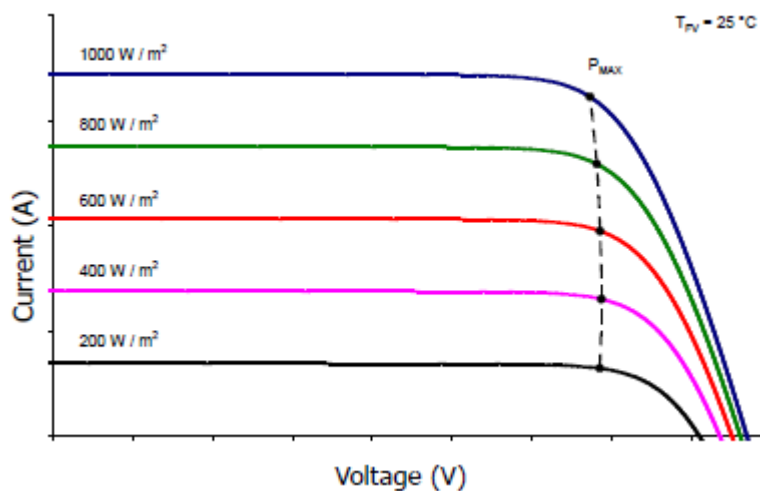


Figure 3.2 Irradiance effect on I-V curves

- Dependence on temperature: as temperature increases,  $I_{sc}$  increases and  $I_{mpp}$  decreases,  $V_{oc}$  and  $V_{mpp}$  decrease significantly due to increment of  $I_0$ :

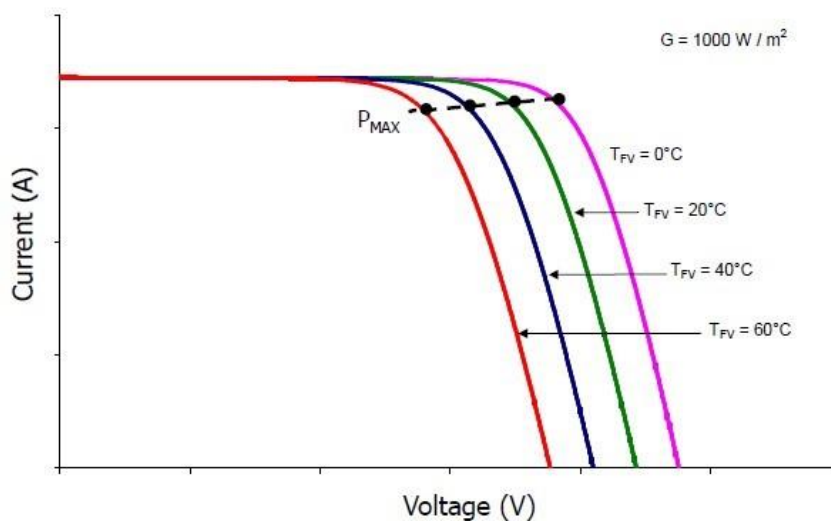


Figure 3.3 Temperature effect on I-V curves

Loads need values of current and voltage higher than those necessary to a single cell, for this reason it must connect many cells in series or in parallel.

This connection can cause mismatch in the current-voltage curves. For example if  $N_s$  cells are series connected and one has I-V curve different from the other curves, the total I-V characteristic is obtained by the sum, for each value of current, of the voltage  $(N_s-1) \cdot V$  of the good cells with the voltage of the weak cell. This causes an important consequence,  $P_{max}$  is much lower than the expected power  $(N_s-1) \cdot P_{max}$ .

The just made consideration shows that it is necessary to use cells with I-V curves as similar as possible: this requires a precise selection of the cells in the manufacturing (cells with equal values of  $I_{sc}$ ,  $V_{oc}$ , and  $P_{max}$  should be connected). Regretfully during the plant operation, even if an accurate selection is performed, it is impossible to avoid the I-V mismatch due to external reasons.

## 3.2 Electroluminescence

Electroluminescence (EL) is particular kind of luminescence that characterizes some materials able to emit light when current flows inside, i.e. under electric field action. It is the consequence of electrons and holes recombination in a material, in particular in semi-conductors. This emission is detectable by an appropriate camera.

In photovoltaic sector, EL-test is implemented in modules' quality control, both before installation and during their operation. Electroluminescence imaging is non-

invasive and must be conducted in laboratory (due to the need of testing in a dark environment) so, during operation phase, it means a lack in plant power production, which is why test duration should be as short as possible. .

Using this kind of maintenance operation, it is possible to detect cell cracks in photovoltaic modules, since they appear as dark lines. An operator able to recognize these lines, since this function has not been automatized yet, must perform the test.

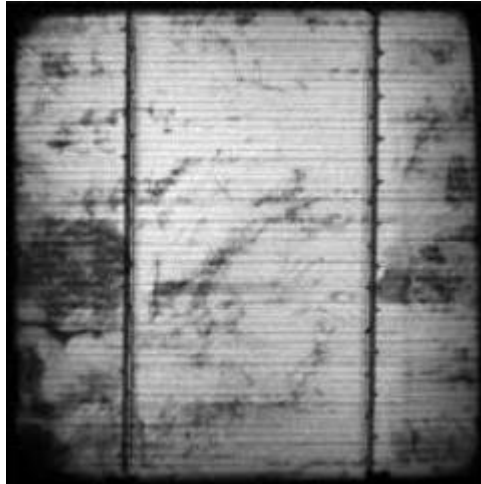


*Figure 3.4 Cell crack detected by electroluminescence*

Being performed only in laboratory, this test is rarely carried out during plant operation. This test is useful for PV modules producers when the customer complains of frequent breakage of the products, in fact it can help in clarifying the root causes of this anomaly.

### 3.3 Visual inspection

Visual inspection represents the fastest method to detect failures in PV module, so it could be introduced for new modules being tested in STC as described in the standards [IEC61215, IEC61646].

Typically, in pre-installation phase, this kind of inspection is carried out before and after the module has been subjected to stress testing in laboratory. During the operation period, modules are subjected to controls with constant frequency, as a maintenance routine operation. For this reason, it is possible to distinguish the two different tests with the respective results.

### 3.3.1 Visual inspection in laboratory

In laboratory, the panel is commonly subjected to thermal cycling, mechanical loading, damp heat exposure, humidity-freeze cycling, UV irradiation, hail impact, outdoor exposure, and thermal stress. This is functional to the choice of the best design.

Listed below, typical failures found in laboratory:

- bubbles or delamination of the front of the module;
- cracked or burned cells;
- bend, broken or scratched frame;
- oxidised or corroded junction box;
- damaged back of the module;
- exposed electrical parts for issues in wires.

### 3.3.2 Visual inspection in the field

During the operation phase, this kind of inspection is a great tool to identify causes of failures of PV modules or to identify problems that could cause failures in the future. Not all the problems are visible: sometimes module has internal issue not detectable with visual inspections. This is useful to identify burn marks, delamination, encapsulant yellowing, junction box failure, and many others.

The same errors of the previous list can be found. They will be better analysed in the following chapter basing also on the safety risk they cause.

## 3.4 Thermography

Thermography is one of the most used methodologies of maintenance of photovoltaic plants, but not everyone knows that three different types of thermography exist. The pulse thermography and the lock-in thermography are lesser known because they need to be performed under lab conditions so they are rarely carried out, even if they allow a very detailed view into the PV module. The thermography under steady state conditions is the most common because it allows to perform the analysis in the field under working conditions.

### 3.4.1 Pulse thermography

The pulse thermography needs an external heat source to generate a dynamic heat flux through a PV module, an example are one or more simultaneous triggered powerful flashlights. The pulse must last only few milliseconds not to have unclear images. The flash has to be located in front of the module and its intensity should make the surface temperature rise immediately about 1 K to 5 K equally. After excitation, the surface temperature decreases and a thermographic camera with a high repetition image acquisition frequency takes constantly images.

From the analysis of these images, an inhomogeneous distribution of the material's heat capacity and thermal conductivity can be detected, because this affects the evolution of the temperature distribution. The results are good, but in addition to being carried out in laboratory, this kind of thermography has another disadvantage: it requires a camera system with high speed and high resolution, expensive qualities.

### 3.4.2 Lock-in thermography

Lock-in thermography, along with pulse thermography, must be performed in laboratory. During LIT the module is excited at a controlled frequency, enhancing the signal to noise ratio, so that also weak heat sources can be perceived.

To achieve an excellent result in this test, cooled IR-camera and uncooled bolometers are required. Thanks to the periodic excitation of the samples coordinated with the image recording, thermal differences in the range of 10  $\mu$ K can be made visible.

The cell can be excited in two different ways:

1. Dark lock-in thermography (DLIT): measurement performed applying an electrical current or voltage source;
2. Illuminated lock-in thermography (ILIT): test is carried out using a light source. This is a very good solution because it is totally contactless and so it can be performed at an early manufacturing stage.

### 3.4.3 Thermography under steady state conditions

Thermography under steady state conditions is the only way to effect thermography outdoor, during plant operation. It represents a frequent operation in a PV plant maintenance and is an excellent test to control modules conditions.

To have optimal result this test must be performed on a sunny cloudless day, with a minimal irradiation of  $700 \text{ W/m}^2$  (for this reason it lasts 4-5 hours a day). The temperature distribution can be measured by way of an appropriate thermal camera, able to make IR images; its angle of view should be set as close as possible to  $90^\circ$  but not less than  $60^\circ$  to the module glass plane.

When illumination is uniform, cell temperatures should differ by only few degrees. If defects are present, these temperature variations may be much larger reaching delta of temperature equal to multiple of 10 K, indicating the presence of hot spots.

This kind of thermography will be deepened following, considering an automatized version.

## 3.5 Robotization in O&M

Like all work sectors, also the energetic one, and in particular the photovoltaics, is going through a phase of robotization, so as to make daily operations more and more economical and faster, often succeeding in increasing the sustainability of processes. Particularly for large utility-scale the need to contain costs and, at the same time to maintain a good efficiency, has arisen.

Among the numerous innovations, particular attention is given to those one useful during the operation and maintenance of the photovoltaic fields. The following is an analysis of some.

### 3.5.1 Exoskeleton

The exoskeleton technology is a passive upper-limb exoskeleton capable to assist workers' shoulder flexion-extension, mainly in tasks of overhead manipulation. This is very similar to those ones diffused in automotive industry.

A plausible application scenario of the exoskeleton is reported in figure, which shows an operator during maintenance or assembling operations.



*Figure 3.5 Plausible application scenario of the exoskeleton*

It is important to underline that this is a passive device, so it just support the operator improving his work conditions but does not increase his arm power.

### 3.5.2 Smart glasses

The main benefit of this technology is the possibility to have remote assistance: the operator in field is in contact with an operator who supports him from anywhere in the world and contemporary he has hands free, able to work and repair the failure.

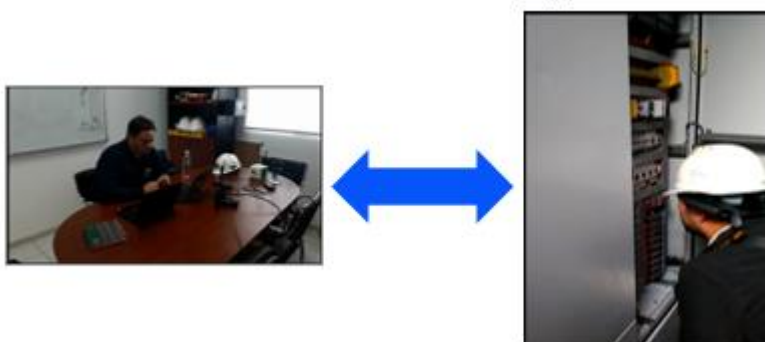


*Figure 3.6 Plausible application scenario of the smart glasses*

This allows understanding better what happens in field, in particular when the photovoltaic plants are far from central headquarter. The most advanced version contains software that, basing on the detected image, recognizes the fault and gives instructions on how to repair it to the operator.

### 3.5.3 Cleaning machine

Soiling is an important issue regarding PV module power output and consequently cleaning is a fundamental maintenance operation. Unlikely the areas most affected by this problem are also those where there is scarcity of water availability, for this

reason it is essential to study dry solutions that reduce or even cancel the use of water.

There are different cleaning machines which satisfy this need and they exploit different technologies:

- Air pressure
- Dust suction
- Rolling brush
- Rotating brush
- Air pressure + rolling brush
- Air pressure + static brush
- Dust suction + rolling brush
- Dust suction + static brush



*Figure 3.7 Example of cleaning machine*

Each robot works moving over the PV panels by the mean of wheels of approximately 10 cm of diameter, which give the robot the axial movement, and other wheels are in upper and lower end to stabilize it.

It is a solution without the use of water, and autonomous in term of electrical feeding due to its on-board PV panel and batteries, the cleaning is done using

rotating brushes like car-wash systems, that would not damage the panel surface or brushes. It is programmable in terms of working time and speed.

### 3.5.4 Grass cutting machine

This can seem a simple project to develop, but some issues makes this machine difficult to implement.

Photovoltaic plants are usually located in remote zones, on uneven terrain and sometimes with some slope. In addition, the grass can be very high and brush usually grows between the series of panels compromising PV park power output. The machine could also become home to snakes, mice and other nature.

Facing these problems, the best solutions for the time being is a remote controlled robot, so not completely autonomous.



*Figure 3.8 Example of grass cutting machine*

Another possible solution is the use of tractors that, once memorized the pathway, can repeat it every time needed.

### 3.5.5 Drones



*Figure 3.9 Drone flying over a PV field*

In this contest of robotization the use of Unmanned Aircraft System (UAS), well known as drones, is developing.

Most UAS can be divided in two main categories, basing on flight architecture:

1. Rotor-based: small, light and easy to control;
2. Fixed-wing: fly at higher altitude, are faster and carry heavy loads.

The first category anyway, is the most diffused one since it has taken the franchise thanks to low prices and high reversibility.

These devices can currently perform a variety of PV-related tasks, including visual imaging (of modules, wiring, and other plant components), infrared thermography, and vegetation monitoring that have the potential to update largely manual conventional processes and more efficiently identify and diagnose PV system performance issues. Moreover, future UAS capabilities, such as data analytics through pattern recognition and change detection, offer greater potential economic upside by introducing predictive methods for gauging plant health and optimizing strategic O&M responses.

This kind of technology is in continuous evolution and, for this reason, its cost is really affordable. The main values include:

- Time savings and labour efficiency: drone can complete determined tasks, such a PV plant survey, faster and inexpensively than traditional approaches;
- Increased accessibility and safety: UAS can gain access to locations difficult for men to reach, or that pose safety risks, i.e. rooftops;
- Flexible dispatch: due to their marginal cost and to low transport cost, these little aircrafts can be dispatched on as-needed basis;
- Enhanced data collection: UAS allow many types of data to be collected, often simultaneously, and at a faster rate. This paves the way for a better predictive maintenance, avoiding to incur n failures before they happen;
- Greater accuracy: measurements taken via UAS imaging for rooftop and ground assessments, as well as other applications, can offer improved accuracy over manual methods.
- Application stacking: the flexibility of the UAS platform allows a single device to perform a variety of applications.

This speech can be incorporated in a robotization process concerning not only PV fields, but every kind of plant, using renewable or non-renewable energy sources.

In EGP the drones are used in all technologies plants: hydro, wind, solar, geo. They are principally used to make inspections with supported cameras.

This study is focused on the use of UAS in photovoltaic fields during maintenance operations, analysing technic and economic aspects of their implementation. For the time being their utilisation is confined to thermographic and visual surveys.

Starting from experimental data and from on field experiences, all PV plants' needs have been set, choosing the best hardware and software for the requested analysis.

The following scheme summarises the entire process, from the collection of the images to their analysis.

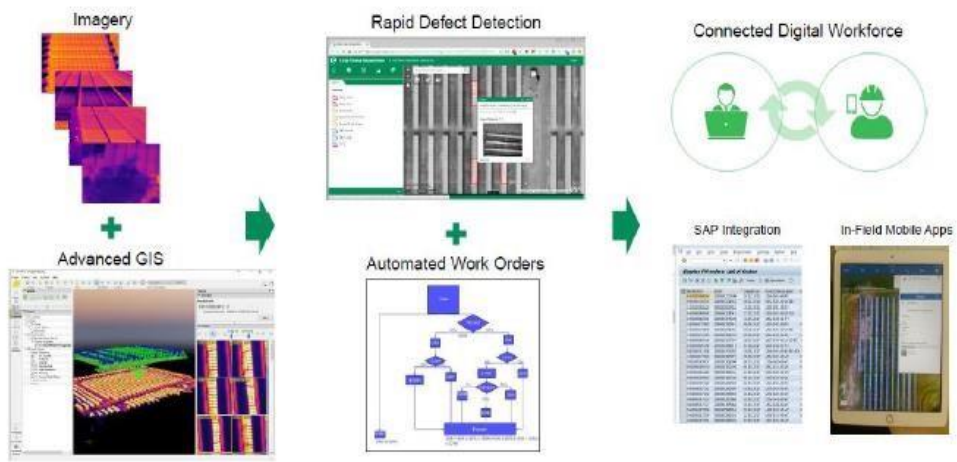
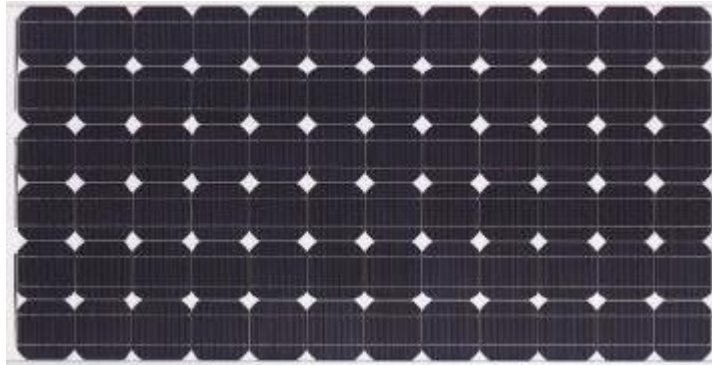


Figure 3.10 Automated thermography process

# 4 Polycrystalline modules failures

## 4.1 Polycrystalline module

A photovoltaic module is composed of several solar cells, connected in series or in parallel, characterised by an important parameter, the energy gap.



*Figure 4.1 PV module with 72 solar cells in series*

A solar cell can be made of different materials. Each of them has its own value of energy gap, efficiency and a corresponding surface area required for 1 kW.

Following the most used:

Technology	Energy gap [eV]	Efficiency [%]	surface required for 1 kW [m <sup>2</sup> ]
Mono-crystalline Si	1.17	15-21	5-7
Poly-crystalline Si	1.12	14-16	7-8
Amorphous Si	1.75	6-10	10-17
CIS thin-film	1.05	13-15	7-10
CdTe thin-film	1.45	11-13	7-10

*Table 4.1 Different PV cell technologies*

The main components of a PV module are:

- Front glass with 3-4 mm thickness;
- Glass or tedlar back-sheet;

- Solar cells encapsulated by Ethylene Vinyl Acetate (EVA), a hot-melt adhesive with waterproof properties.
- Aluminium frame;
- Junction box.

The solar cells are connected by ribbon connections, which are joined to the main bus-bars and to the back electrode of the adjacent cell. Connection terminals are placed in the junction box where there are also by-pass diodes.

This study will focus on poly-crystalline modules, the most diffused type of panels nowadays.

The poly- crystalline ingot technology is called "block casting": the silicon, through the electricity, is fused into a graphite crucible, then a controlled cooling with crystallization is executed. Silicon crystals are vertically aligned to the surface and, through a slice, parallelepiped square-based ingots are obtained; both top and tail of the ingot are removed, due to the large content of impurities. The material has a boron-based (P-type) doping.

Finally, ingots are cut into slices by multi-wire diamond saws, obtaining a wafer of 0.2-0.3 mm thickness; unfortunately, 30-50% of the material is lost after sawing. The result of all this process is cells with a mosaic appearance.

Panels composed by this kind of cells are cheaper and less efficient than monocrystalline ones, but their durability is comparable.

Year by year PV modules become cheaper and this trend does not seem to stop; the following graph shows this variation from 1976 to 2018.

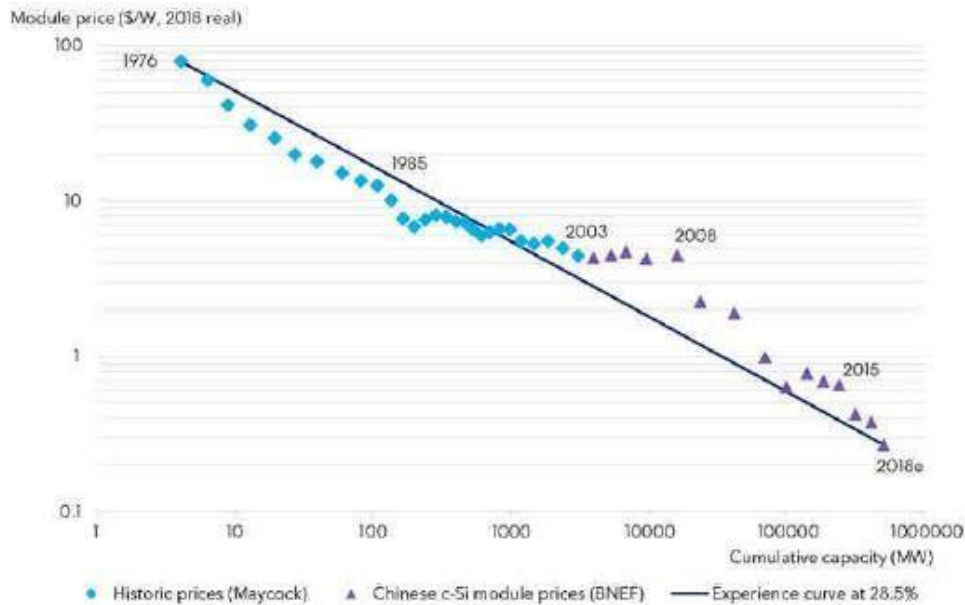


Figure 4.2 Module price over the years

This curve describes a learning rate of about 28.5%, it indicates the cost reduction per doubling of deployed capacity.

## 4.2 Definition of failure

Firstly, there is the need to define what a PV module failure is. In this contest, a PV module failure occurs when something causes power loss at the panel. Anything else that does not lead to this consequence has not been considered here. At the same time, faults caused by natural disasters or extraordinary climatic conditions have not been taken into account, but only failures which arise under normal conditions.

The following formula helps to understand if a power loss is occurring:

$$P_m + \Delta P_m < P_1 - \Delta P_1$$

$P_m$  = module power measured under conditions stabilized in IEC 60904

$\Delta P_m$  = total uncertainty of the measurement

$P_1$  = power printed on the module

$\Delta P_1$  = tolerance stated on module label

Hence, when the expected power minus the tolerance are bigger than the measured power plus the uncertainty a power loss failure occurs.

Power loss can depend from different factors; it usually increases with temperature, voltage, current, humidity, mechanical load, UV irradiation, thermal cycling and shading.

The International Energy Agency, in its *Review of failure of PV modules*, provides a categorization of different failures basing on power loss associated.

Power loss category	Description
A	Power loss below detection limit <3%
B	Exponential-shaped power loss degradation over time
C	Linear-shaped power loss degradation over time
D	Power loss degradation saturates over time
E	Degradation in steps over time
F	Miscellaneous degradation types over time

*Table 4.2 Power loss category*

Another fundamental aspect for failure categorization is the safety issue it brings; IEA has also set a risk scale made of three levels:

- Level 1: failure has no effect on safety and no significant losses;
- Level 2: failure has indirect effect on safety and no significant losses;
- Level 3: failure has direct effect on safety and no significant losses.

A further restriction is set: the deepened failures are those ones detectable by thermography and visual inspection; they have been split in physical and thermal anomalies, the first ones easily detectable by visual images, while the second ones by a thermal camera.

## 4.2.1 Physical anomalies

### 4.2.1.1 Shattering

Cells are made of silicon and this makes them breakable. The first issues occurs during manufacturing process: here the first cell cracks can arise and, in this phase, most of them are not visible to the naked eye since they are in silicon substrate. Later also during PV module production cracks can occur during cells assembly

Other issues rise up during the plant construction phase: transport and installation cause many glass breakages. This can depends both from the planning and from the operators in field during clamping phase: the panels are installed in such way to suffer not expected stresses.

During operation of the solar module the risk that short cell cracks can develop into longer and wider cracks increases. This is because of mechanical stress caused by wind or snow load and thermos-mechanical stress on the solar modules due to temperature variations caused by passing clouds and variations in weather.



*Figure 4.3 Example of shattering*

Shattering occurs when the glass is cracked, the first phase is usually cell cracks. If a crack separates a part from a solar cell, this cell is driven in reverse bias and will dissipate power. This defect will only lead to abnormal heating if the size of the separated part is larger than 10% of the cell size. The leakage current across the remainder part of the cell may not be uniform but concentrated to certain areas. Accordingly, abnormal heat generation cannot be predicted. Different kinds of crack exist and they do not represent an immediate dangerous situation, but they can evolve into worst situations (severity level 1, loss production grade D)

Secondary effects are due to crack patterns: if a zone >10% of the cell area is electrically separated, the cell will be operated under reverse bias, followed by areal heating. This will accelerate any temperature driven degradation mechanisms, such as formation of acetic acid, which will cause EVA browning. Micro-cracks in this cell area will enhance diffusion of oxygen causing photo-bleaching around the micro-cracks.

Most critical are cracks parallel to bus bars. Accidental contact between the separated and active cell parts can lead to localized current flow and arcing, which will cause hot spots and burn marks.

#### 4.2.1.2 Soiling



*Figure 4.4 Example of soiling*

Soiling literally means “dirty panel”: the causes can be different but the main are bird dropping and dust. The consequence are loss in production and activation of bypass diode. It has a severity level 1 and power loss grade C.

#### 4.2.1.3 Snail tracks

The name of this failure derives from similarity between the effect obtained on the module and the wake left by the snails, a darkening of the area concerned. An example in the image below.



*Figure 4.5 Example of snail track*

A snail track is a discolouration of the silver paste used for the gridlines of the solar cells that usually appears at the edge of the cell or along cell cracks.

The cause of this failure is not clear yet, but it has been noticed that in this discolouration along the silver finger of the front side cell metallisation shows nanometer sized silver particles in the EVA above the silver finger. These silver particles (always in compounds: sulphur, phosphorus or carbon) cause the discolouration. The affected fingers are more porous, leading to a reduction of the conductivity.

Snail tracks can be a consequence of cell crack and humidity: this enters in the module from the backsheet end propagates through the cracks, causing the

oxidation of silver finger. In addition, the choice of materials is important, in particular of those that compose encapsulant and backsheet.

The sure consequence is that PV modules being affected by snail tracks show a tendency to high leakage currents. The severity level can be set at 2, and the loss production grade at C.

#### 4.2.1.4 Burn marks

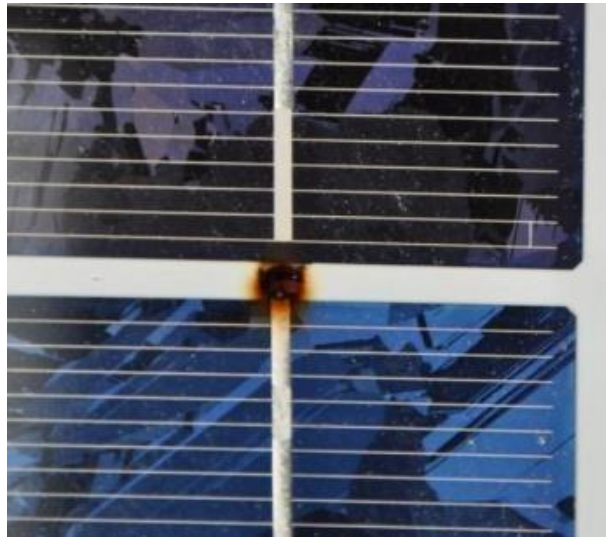


*Figure 4.6 Example of burn marks*

This defect occurs when a part of the module becomes very hot, causing a permanent burn mark that often lead to power losses (severity level 2, loss production grade D/E).

One cause is associated to welds and connections subjected to thermal fatigue. In this case, the resistance increases with the temperature until this one is high enough to discolour front and back encapsulation.

Another case of burn mark is that one caused by a cell forced into reverse bias because shaded; the reverse current flow causes heating, hence thermal stress and finally burn mark.

These faults can usually be identified through visual survey and they often require module substitution, to be sure it is necessary a thermographic analysis.

#### 4.2.1.5 Delamination

The adhesion between galls, encapsulant, active layer and backsheet can be ruined for many reasons.

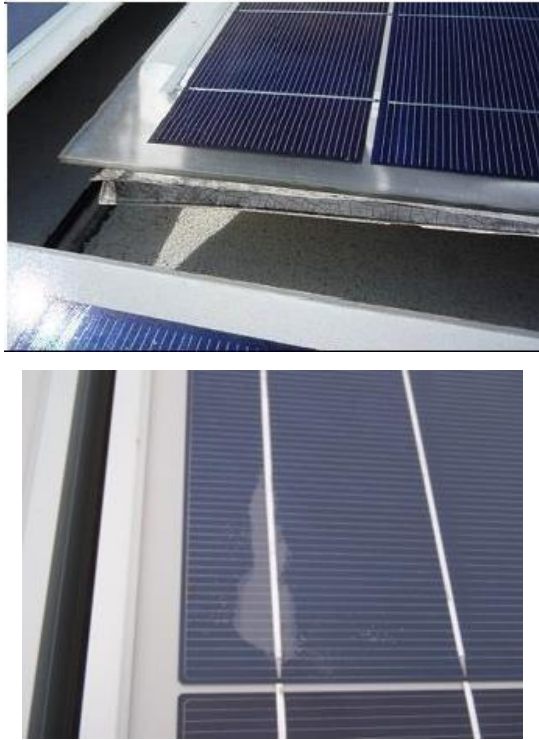


*Figure 4.7 Examples of delamination*

It is typically caused by weakening of bond strength (figure up) and by low adhesion at interfaces due to material incompatibility (figure down).

The consequence of delamination are:

- bubbles, creases or imperfections on the plastic rear surface;
- production of less current in the delaminated area;
- if current mismatch is significant it will trigger the bypass diode and cause further power loss;
- it allows air and moisture to creep inside, causing corrosion and imminent failure.

In most of cases, it is necessary to change the modules, to avoid both further output losses and electrical hazards (severity level 2, power loss grade D/E), but sometimes, if not excessively delaminated, and only after a detailed evaluation, some panels could possibly be recycled in -installations with low tension.

To prevent delamination, “gel content test” could be performed before installation in order to confirm the quality of the EVA and minimize the risk of delamination.

## 4.2.2 Thermal anomalies

These anomalies are detectable through the proper thermal camera. Based on the camera and the software used, different values of delta of temperature are detectable.

In most of cases, the thermal fault is named “hot spot”: this means that in a specific point of the module temperature is higher than in the rest of the panel, this can regards one single cell or more cells. Beyond “hot spot” there may be lots of failures that will be examined now.

### 4.2.2.1 Electrical mismatch

The PV module have cells interconnected in series with ribbons, forming string, to obtain higher module output voltage. The strings, in turn, are interconnected in series or in parallel by interconnections.

In this intricate system of interconnections, it may happen to have a cell or/and string interconnection weaker than others. During transport, installation or operating phases this interconnection can break causing electrical mismatch.

The disconnected cells become warmer than others and are detectable by IR camera.

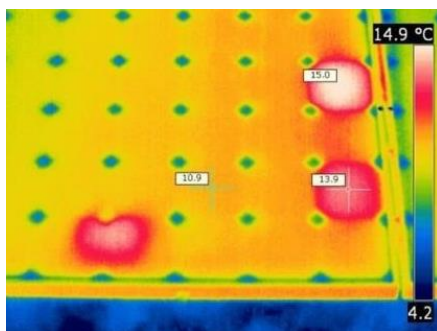


*Figure 4.8 Example of electrical mismatch*

In this first phase of the problem safety risk is almost absent but associated to other failures, and after a period of time, it can cause serious consequence, like glass breakage and burn marks on the backsheet.

Hence, for the potential consequences, severity level is 3 because it can cause fire and be dangerous for operators in field, while loss production grade is E.

#### 4.2.2.2 Shadowing and activated bypass diode

The shadowing is more frequent than one might think; it usually is caused by vegetation, design errors or trackers failure. In these cases bypass diode takes action.



*Figure 4.9 Example of shadowing*

Theoretically, for best efficiency of the system, every cell should be connected to one diode, but to simplify the production process and contain the costs of the modules the manufacturing industries usually put 2 or 3 diodes in one module, up to its geometry. Bypass diode is put in parallel to a certain number of in series cells into the PV module and when one or more cells are shaded, it intervenes to reduce the consequent power loss.

This cell stops generating current and in turn becomes a load by reversing its polarity and absorbing the electrical energy produced by the other cells with the effect of heating up. In these cases, the passage of reverse current through the shaded cell (hot spot) can be avoided through a by-pass diode: the diode intervenes, bypassing the darkened cell and all the cells belonging to that area.

A thermography can easily detect this situation, since the whole interested area is excluded and has a temperature different from the adjacent zone (safety risk level 2, power loss constant).

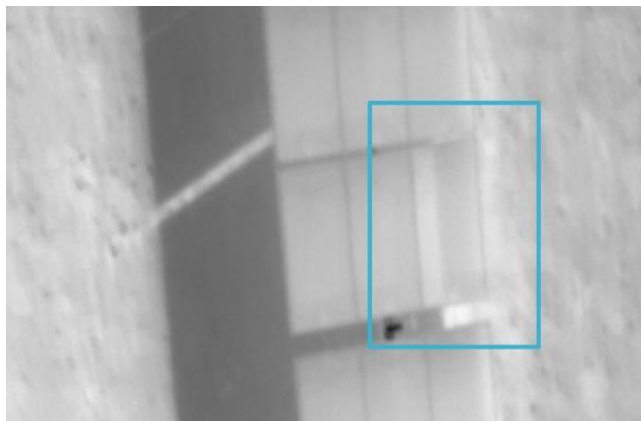


*Figure 4.10 activated bypass diode through thermography*

It can also happen that a bypass diode fails. In this case it becomes a little resistance and become hot causing little burn marks on the back of the backsheet, so it is more difficult to identify the bypass diode failure than its activation.

#### 4.2.2.3 Potential Induced Degradation (PID)

This can be considered a “young” module defect, in fact, it has been noticed only in the last decade. Actually this fault has been present in literature since 1970, but it was never been verified in field. This is due to the born of very big photovoltaic plant in which the output transformer in the inverters is often eliminated.

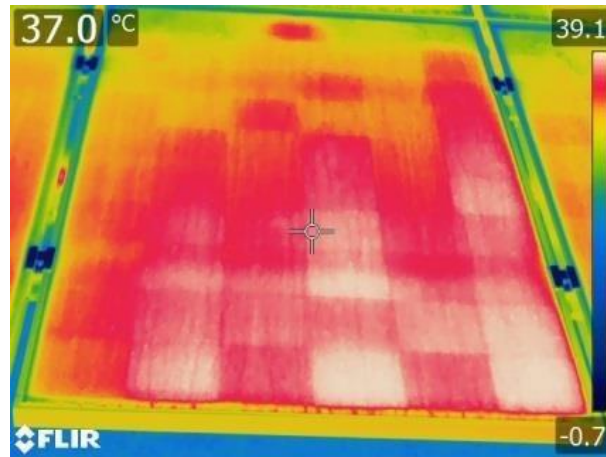


*Figure 4.11 Example of PID*

In June 2011, the Fraunhofer Center for Silicon photovoltaics published the results of a test, according to which the PID is responsible for a power reduction of almost 70%.

One way to detect PID is through thermography: from the cell colour of each individual module, it is possible to distinguish between healthy and diseased modules: cooler yellow cells, therefore healthy, warmer orange cells, therefore affected by PID. This test must be done in full sunlight and does not interfere with the operation of the system but does not give any indication of the level of degradation of the cells or the percentage of power lost. A severity level 1 and a loss production grade C can be associated to this fault.

When a PID issue is found, loss of performance is valued (how much is the loss of energy), electroluminescence analysis is performed (unfortunately often this must be done in the laboratory) and if it is necessary to make a correction, an anti PID device (such as PidBull, Grounding Kit, etc.) is installed.

This device is inserted into the inverter and acts over everything connected to it. Unfortunately, every module damaged by PID must be substituted, recovery is not possible.

#### 4.2.2.4 Encapsulant discolouration

The most used encapsulation material is EVA (ethylene vinyl acetate) and its discolouration represents one of the most frequent mechanisms of module degradation.



*Figure 4.12 Example of EVA discolouration*

Additives, among which UV and thermal stabilizers, compose EVA and the choice of materials is very important. If additives and their concentrations are not suitable, once in field, the EVA may discolour and this lead to various consequences.

When the choices are wrong, the materials subjected to UV rays, undergo a process of yellowing (named browning). Eva transmittance can go from initial values typically >90%, to values <80%. In addition, at high temperature, EVA deteriorates into acetic acid, which reacts with silver of the contacts and with welds, favouring the increase of dispersion currents and a reduction of capacity to collect charges by the contacts themselves.

Glass can have an important role in protection from UV rays, with good impacts on encapsulant and cell stability.

Typically, the ruined cell is at higher temperature than the surrounding cells of the module (so it is detectable by thermography). If restricted to one cell, it does not represent a safety risk (safety risk 1) but it can cause a faster degradation of cell and module with a consequent surface corrosion (loss production grade C).

# 5 Guidelines for the use of drones in the field

The first drone implementation has taken place in Enel Green Power North America: this is the first country that has used the UAS to perform visual inspections and thermography.

Based on their experience, every Country needs have been estimated according to plants dimensions: flight time and number of useful drones. This has been done in anticipation of the conclusion of the contract with Raptor Maps, to determine the costs to be incurred.

## 5.1 Countries management

In USA 179 MW have been inspected and the acquired knowledge is shown here:

1. Flight time: 8 MW/hour. This value is mediated between image quality and inspection duration considering also battery change;
2. Setting up and breaking down last about 1 hour;
3. Number of ideal drones: 1drone/100MW, i.e.  $0.5\text{drone}/\text{km}^2$ . This value comes from some considerations: one drone should be shared among plants (of the same Country) lower than 30 MW if distances allow it, one drone should be bought for plants large 30-100 MW and more than one drone for plants larger than 100 MW.

The following table resumes needs of each Country.

Country	Installed MW	Number of drones
Australia	200	2
Brazil	1291	7-8
Chile	492	6-8
Colombia	86	1
Greece	87	1
Mexico	1211	9
Panama	49	1

Peru	179	1-2
Romania	36	1
South Africa	323	4
Spain	352	3-4
USA	179	3

*Table 5.1 Useful drones for each Country*

At this point, it has been necessary choosing from the wide range of products available on the market the best asset drone-camera functional to the purpose.

## 5.2 Choice of drone

For what concerns the choice of drone Enel has decided to rely on one of the best production companies, DJI. Headquartered in Shenzhen, widely considered China’s Silicon Valle, it is a high-tech manufacturing facility specializing in unmanned aerial vehicles.

Differing from other technologies, drones aimed at photovoltaic fields surveys do not require high technical characteristics. The route to be followed is a 2D pathway and flying height never exceeds 150 meters, contrary to what happens during wind turbines inspection. Here the drone is obliged to flight at very high heights, where it must withstand the high force of the wind, following a 3D pathway to analyse the entire blade profile.



*Figure 5.1 Drone during a wind turbine inspection*

For this reason, choosing the best drones for PV surveys does not require elevated costs, the following table contains a selection.

<b>DRONE (DJI PRODUCTS)</b>	 <b>MATRICE 600 PRO</b>	 <b>PHANTOM 4 PRO</b>	 <b>MAVIC</b>	 <b>MATRICE 210</b>	 <b>MATRICE 100</b>
<b>STANDARD BATTERY</b>	Lipo 6s; capacity 4500 mAh	Lipo 4s; Capacity 5870 mAh	Lipo; capacity: 3850 mAh	Lipo 6s; Capacity 4280 mAh	Lipo 6s; Capacity 4500 mAh
<b>DIAGONAL WHEELBASE (mm)</b>	1133	350 (propellers excluded)	335 (propellers excluded)	643	650
<b>DIMENSION (unfolded) (mm)</b>	437 x 402 x 553	/	83 x 83 x 198	887 x 880 x 378	355 x 254 x 254
<b>WEIGHT (Kg)</b>	9.5	1.375	0.743	3.84	2.355
<b>MAX TAKEOFF WEIGHT (Kg)</b>	15.5	/	/	6.14	3.6
<b>MAX PAYLOAD (Kg)</b>	6	/	/	2.3	1
<b>HOVERING ACCURACY</b>	<b>VER</b>	± 0.5	± 0.5	± 0.5	± 0.5
	<b>HOR</b>	± 1.5	± 1.5	± 1.5	± 2.5
<b>MAX WIND RESISTANCE (m/s)</b>	8	10	10	12	10

<b>MAX SPEED (Km/h)</b>		65	72	65	80	61
<b>MAX FLIGHT TIME (min)</b>	<b>NO PAYLOAD</b>	32 with 6 batteries	30	31	27 with 2 batteries	22
	<b>FULL PAYLOAD</b>	16 with 6 batteries	/	/	13 with 2 batteries	13
<b>OPERATING TEMPERATURE (°C)</b>		-10 TO 40	0 TO 40	0 TO 40	-20 TO 45	-10 TO 40
<b>MAX TRASMISSION DISTANCE (Km)</b>		5	7	8	7	5
<b>VIDEO OUTPUT PORT</b>		HDMI, SDI, USB	HDMI, USB	HDMI, USB	HDMI, USB	USB, Mini-HDMI
<b>PRICE (€)</b>		5699	1699	999	10000	3599
<b>ASSOCIATED CAMERA</b>		Compatible with multiple cameras	On board camera	On board camera	Compatible with multiple payloads	Compatible with X-3 camera and gimble

*Table 5.2 Drones selection*

One of the biggest problems that occurs when using a drone is the time flight: the batteries use do not allow a long autonomy and this leads to buy more spare batteries and to loose time for changing them during the inspection. Furthermore, many drones fall down when discharged without prior notice causing their breakage but also a potential safety risk for the pilot driving in that moment.

As a result, many new drones have a battery intelligent system, usually composed by more than one battery, capable to send an alarm to remote controller when one of them is discharged and to continue its flight also in this condition.

Among the selected drones, as a result of field trials, the recommended one is “Matrice 600 Pro”, anyway the Countries are able to buy that one they think is appropriate to use.

### 5.3 Choice of camera

The table below compares different cameras, establishing a ranking basing on required technical specifications. The features highlighted in green represent the perfect characteristics, the ones in yellow the acceptable and the ones in red the not appropriated.

Suitable	Model	Spectrum	Radiometric	Resolution	Thermal Lens	Thermal HFOV	Gimbal Stabilized
<u>Preferred</u>	<u>DJI XT2</u>	<u>Thermal + RGB</u>	<u>Yes</u>	<u>640 x 512 + 12MP</u>	<u>13mm or 19mm</u>	<u>45° or 32°</u>	<u>Yes</u>
<u>Preferred</u>	<u>DJI XT-R</u>	<u>Thermal</u>	<u>Yes</u>	<u>640 x 512</u>	<u>13mm or 19mm</u>	<u>45° or 32°</u>	<u>Yes</u>
<u>Preferred</u>	<u>FLIR Vue Pro R</u>	<u>Thermal</u>	<u>Yes</u>	<u>640 x 512</u>	<u>13mm or 19mm</u>	<u>45° or 32°</u>	<u>Custom</u>
<u>Preferred</u>	<u>FLIR Duo Pro R</u>	<u>Thermal + RGB</u>	<u>Yes</u>	<u>640 x 512 + 12MP</u>	<u>13mm or 19mm</u>	<u>45° or 32°</u>	<u>Custom</u>
<u>Preferred</u>	<u>WIRIS 2nd Gen</u>	<u>Thermal</u>	<u>Yes</u>	<u>640 x 512</u>	<u>13mm or 19mm</u>	<u>45° or 32°</u>	<u>Custom</u>
<u>Preferred</u>	<u>Optris PI 640</u>	<u>Thermal</u>	<u>Yes</u>	<u>640 x 480</u>	<u>18.7mm</u>	<u>33°</u>	<u>Custom</u>
<u>Preferred</u>	<u>SenseFly Duet T</u>	<u>Thermal + RGB</u>	<u>Yes</u>	<u>640 x 512 + 20MP</u>	<u>13mm</u>	<u>45° or 37°</u>	<u>No</u>
<u>Not Preferred</u>	<u>DJI XT</u>	<u>Thermal</u>	<u>No</u>	<u>640 x 512</u>	<u>13mm or 19mm</u>	<u>45° or 32°</u>	<u>Yes</u>

<u>Not Preferred</u>	<u>SenseFly ThermoM AP</u>	<u>Thermal</u>	<u>Yes</u>	<u>640 x 512</u>	<u>9.5mm</u>	<u>n/a</u>	<u>No</u>
<u>Not Preferred</u>	<u>FLIR Boson</u>	<u>Thermal</u>	<u>No</u>	<u>640 x 512</u>	<u>8.7mm or 14mm</u>	<u>50° or 32°</u>	<u>Custom</u>
<u>Not Acceptable</u>	<u>DJI XT-R</u>	<u>Thermal</u>	<u>Yes</u>	<u>336 x 256</u>	<u>13mm or 19mm</u>	<u>45° or 32°</u>	<u>Yes</u>
<u>Not Acceptable</u>	<u>DJI XT</u>	<u>Thermal</u>	<u>No</u>	<u>336 x 256</u>	<u>13mm or 19mm</u>	<u>45° or 32°</u>	<u>Yes</u>
<u>Not Acceptable</u>	<u>DJI XT2</u>	<u>Thermal + RGB</u>	<u>Yes</u>	<u>336 x 256 + 12MP</u>	<u>13mm or 19mm</u>	<u>45° or 32°</u>	<u>Yes</u>
<u>Not Acceptable</u>	<u>FLIR ONE Pro</u>	<u>Thermal + RGB</u>	<u>Yes</u>	<u>160 x 120 + 1.5MP</u>	<u>n/a</u>	<u>55°</u>	<u>Custom</u>
<u>Not Acceptable</u>	<u>FLIR Duo R</u>	<u>Thermal + RGB</u>	<u>Yes</u>	<u>160 x 120 + 2MP</u>	<u>n/a</u>	<u>57°</u>	<u>Custom</u>
<u>Not Acceptable</u>	<u>FLIR Boson</u>	<u>Thermal</u>	<u>No</u>	<u>320 x 256</u>	<u>4.3mm or 6.3mm</u>	<u>50° or 34°</u>	<u>Custom</u>
<u>Not Acceptable</u>	<u>WIRIS 2nd Gen</u>	<u>Thermal</u>	<u>Yes</u>	<u>336 x 256</u>	<u>13mm or 19mm</u>	<u>45° or 32°</u>	<u>Custom</u>

*Table 5.3 Cameras selection*

Let us analyse the most important characteristics a camera must have:

- Both radiometric cameras and not radiometric ones can execute thermography. The latter essentially provide a thermal image showing temperature differences, but it is not possible to measure the absolute value of the temperature on that image. Radiometric thermal imaging cameras instead, allow measuring the absolute temperature value of each point on the image. The image is built on a matrix of a certain number of pixels for a certain number of lines and the instrument's electronics quickly detect the energy stored by each individual pixel of the observed object. More pixels means more detail, since the radiometric thermal imaging cameras are able to detect the absolute temperature for each pixel detected. The correspondent format is radiometric JPEG or TIFF.

- Survey scope is principally collecting thermal images but, to take full advantage of drone's flight, also photographs are taken. This can be executed with a unique camera with thermal and RGB spectrum or with two cameras, one for thermal images detection and one for visual inspection. The first solution is the preferred one: the lower the weight that the drone carries, the greater its battery duration.
- Horizontal Field of view: the angle of view of a photograph or camera is a measure of the proportion of a scene included in the image, i. e. how many degrees of view are included in an image (calculation below).



*Figure 5.2 FoV comparison*

- Gimbal stabilized: this device allows to keep the camera in position despite drone movements.

## 5.4 Raptor Maps

After the choice of hardware, it has been necessary to select a society able to analyse IR images, hence a company owner of the proper software. Among the many realities existing worldwide, Enel Green Power has decided to enter into a contract with an American start up, Raptor Maps.

Raptor Maps was founded by MIT Aerospace Engineers in 2015. It graduated the elite Y Combinator start-up accelerator in 2016 and secured over \$1 million in seed investment. The company recently won the Greentech Media Solar Software Summit start-up competition in 2018.

Raptor Maps is a thought leader in aerial thermography for PV systems, and is frequently hosted by FLIR (global leader in thermal camera technology) and industry trade magazines to share best practices.

Raptor Maps' mission is to build software that brings asset management into the digital age. Their core strengths are machine learning, thermal data, geographic information systems (GIS), and end-to-end software solutions.

Raptor Maps is a global leader in photovoltaic (PV) system analytics, having analysed 2.4 GW of drone-acquired diagnostic PV system data in 2018 and detected over €2 million in previously undiscovered annual production loss. Its customers span six continents and include operations and maintenance (O&M), asset managers, asset owners, engineering, procurement, and construction (EPC), and original equipment manufacturers (OEMs).

Raptor Maps' machine learning algorithms detect, classify, and localize defects. In the image below, the boxes are different colours due to different defect classifications. The boundaries are automatically drawn around the module (as opposed to the defect), so the image can be cropped to the module. Raptor Maps has developed a generic machine learning model for PV systems with a high degree of sensitivity and specificity. Thermal images are pre-processed and normalized.

Raptor maps offers three different levels of survey:

Level I:

- Inverter: Inverter section is offline or significantly warmer than site average
- Combiner: All strings feeding into single combiner box are offline or significantly warmer than site average
- String: Offline string due to circuit interruption or reversed polarity
- Tracker: Tilt tracking mechanism in incorrect or stow position
- Module: Entire module is offline

Level II:

- All anomalies described in Level I
- Module physical anomalies:
  - Shattering: Glass surface of PV system is cracked
  - Delamination: More than 25% of surface of thin-film module is delaminated
  - Soiling and debris: More than 25% of surface of module is covered in opaque substance
- Diode: Activated bypass diode on module

- Hot spot: Clear sub-module thermal anomaly, possibly indicating cell defect, multi-cell degradation, or junction box heating
- Suspected PID: Suspected potential-induced degradation based on site construction and hot spot pattern
- Shadowing:
  - Section of PV system shaded by vegetation (trees and ground cover) at the time of flight
  - Section of PV system shaded adjacent rows at the time of flight
  - Strings shaded by man-made objects (fences, buildings, pylons) at the time of flight
- Weather:
  - Floods and pooling water
  - Damage to rows and tables
- Discrepancies from as-built:
  - Improperly positioned tables
  - Shifted rows due to construction or natural causes
- Site issues:
  - Security issues: Broken fencing, anomalous vehicles, missing equipment
  - Unburied cables: Cabling that represents a safety hazard
  - Access road degradation: Worn road surface, large potholes, vegetation encroachment

#### Level III:

- All anomalies described in Levels I and II
- Analysis in accordance with IEC TS 62446-3 Technical Specification: Photovoltaic (PV) systems – Requirements for testing, documentation, and maintenance – Part 3: Photovoltaic modules and plants – Outdoor infrared thermography. Identification of defects with Class of Abnormality (CoA) 2 and 3.
- Cell: Single-cell hot spot with  $\Delta T > 10$  K
- Junction box: Heated junction box with  $\Delta T > 4$  K
- Substring: Substring in short circuit with  $\Delta T > 4$  K
- Soiling: Module with cells shaded by dirt and  $\Delta T > 10$  K in rainy region and  $\Delta T > 40$  K in arid region.

- Dust: Significant performance degradation due to presence of thin layer of dust. Requires low-altitude, oblique RGB calibration image.

## 5.5 Technical Specifications

Since the inspections will be carried out by Enel Green Power operators in fields, the central O&M has drowned up a *vademecum* about how to perform the activity in order to obtain the right quality of the images. The created document, dubbed “Technical specifications for survey with drone”, has been attached to the Global Framework Agreement with Raptor Maps.

### 5.5.1 Brief resume of the requirements of the thermal sensor

- Radiometric: Captures actual temperature values for each pixel of the image;
- File Format: Radiometric JPEG or TIFF;
- Image Metadata: GPS location, relative altitude, gimbal attitude & timestamp;
- Resolution: 640x480 or higher;
- Refresh Rate: 30Hz or higher preferred. However thermal sensors have export restrictions and only 9Hz may be available in some countries;
- Lens: Horizontal Field of View (HFOV) between 30° and 50° is recommended. 13mm and 19mm lenses are common with FLIR sensors. Just like traditional cameras, the narrower the lens, the wider the field of view of the thermal sensor. The narrower the lens the lower the drone must fly to achieve desired Ground Sampling Distance (GSD).

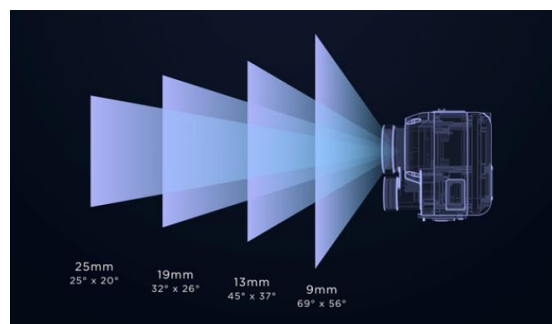


*Figure 5.3 Difference among lenses*

The most important parameter is the ground sample distance (GSD), i.e. the distance between pixel centers measured on the ground.

Type of inspection	Level I	Level II	Level III
GSD	15.0 ± 5.0 cm/pixel	5.5 ± 0.5 cm/pixel	3.0 ± 0.5 cm/pixel

Figure 5.4 GSD for the three levels

### 5.5.2 Recommended annual inspection intervals

	Spring	Summer	Fall	Winter
Typical Site	Level II		Level II	
String Problems	Level II	Level I	Level I	Level I
Module Problems	Level II	Level I	Level II	

Table 5.4 Annual inspections intervals

Level III inspections should only be performed as needed, they are not necessary to be included in annual inspection intervals for most plants.

### 5.5.3 Flight directives

In addition, precise instructions and some hints have been put on paper; for every flight the following procedures must be respected.

For what concerns the pre-flight, before the starting of the thermal inspection, the operator must verify the following conditions:

- Airspace regulations: clear and safe to operate the UAS (drone);
- Equipment check: complete;
- Winds: below 15 MPH (6.7 m/s);
- Skies: Clear & sunny or slightly overcast, Irradiance > 600 W/m<sup>2</sup> is ideal;
- Humidity: Lower is better, Humidity < 60% is ideal;
- Satellite imagery: exists and if satellite imagery does not exist, plan to capture RGB imagery suitable to make a base map;
- Module soiling: non-existent or low.

In case one or more of these conditions will be not respected, the inspection accuracy may be reduced.

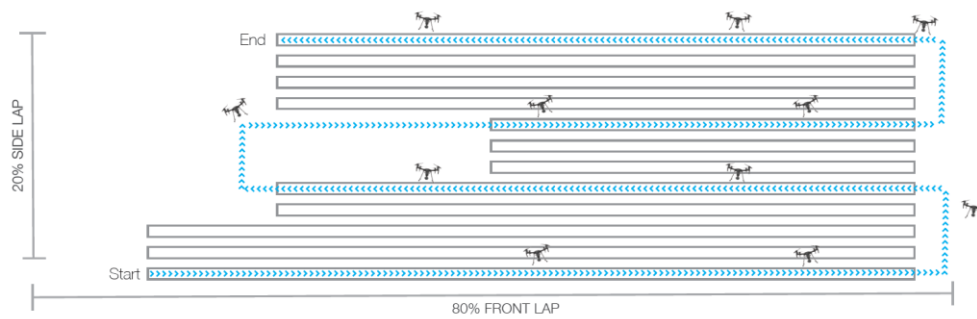
For the flight plan, the pilot must follow the guidelines below, different for thermal and RGB images.

About infrared (thermal) images:

- Flight boundary line: draw around the entire system being inspected and generously extend beyond the edges of the solar farm;
- Flight path: Parallel to the rows of the solar farm;

FLIGHT PATH

Example solar site with drone flight path



Version 3 © 2018 RAPTOR MAPS, INC.

Figure 5.5 Flight path

- Flight Elevation: Maintain consistent elevation above ground level. Terrain with significant elevations changes may require multiple flights and/or advanced ground control software with terrain following capabilities;
- File format: radiometric .jpeg or thermal .tiff (radiometric .jpeg preferred);
- Gimbal pitch: nadir (straight down) with deviation by up to 20 degrees to avoid glare;

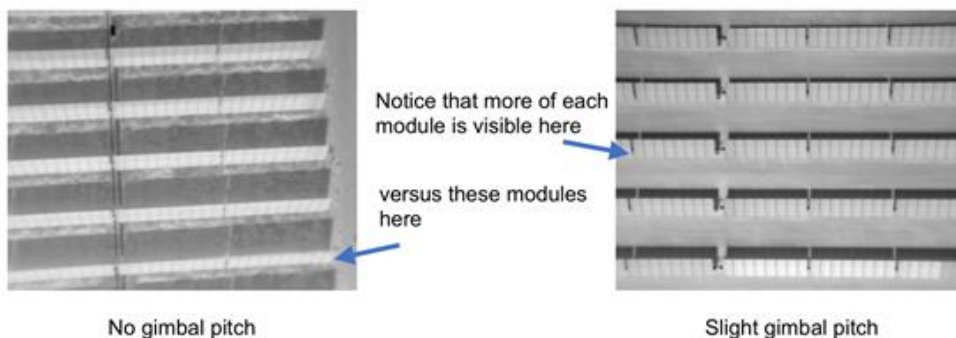


Figure 5.6 Gimbal pitch

- Image capture: Set to auto-capture by time or distance, shutter interval set to 2 second;
- Flight speed: No faster than: Level III (2.5 m/s), Level II (4.0 m/s), Level I (10 m/s);
- Camera ground sample distance (GSD): flight altitude will depend on thermal sensor resolution & lens configuration;
- Front overlap: 80% in the direction of flight;
- Side overlap: 20% over each pass (25% or 30% would be better but considerably increases flight times, 20 is a right compromise);

Inspection Level	GSD (cm/px)	FLIR Lens (mm)	Altitude (m)	Front (%)	Side (%)	Shutter Interval (sec)	Flight Speed (m/s)	Flight Time (min/ha)
III	3	13	23	80	20	2	2	9
		19	33					
II	5.5	13	40	80	20	2	3.5	3
		19	60					
I	15	13	115*	80	20	2	9.7	0.5
		19	170*					

\* Altitudes may exceed local regulations

Figure 5.7 Typical flight parameters

- Camera frame: horizontal edge matches the long edge of the solar rows;

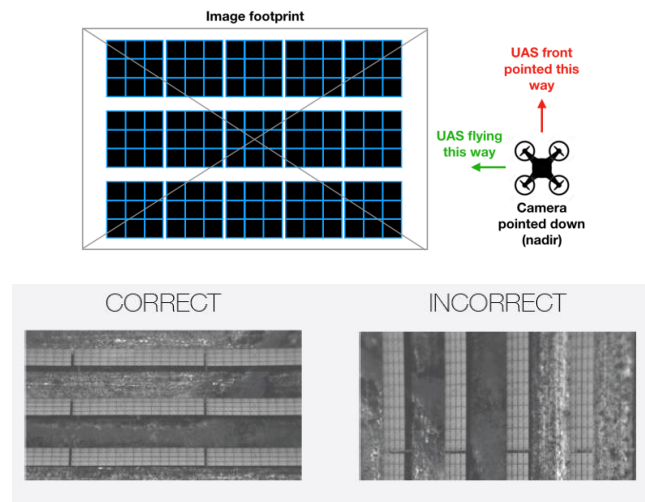
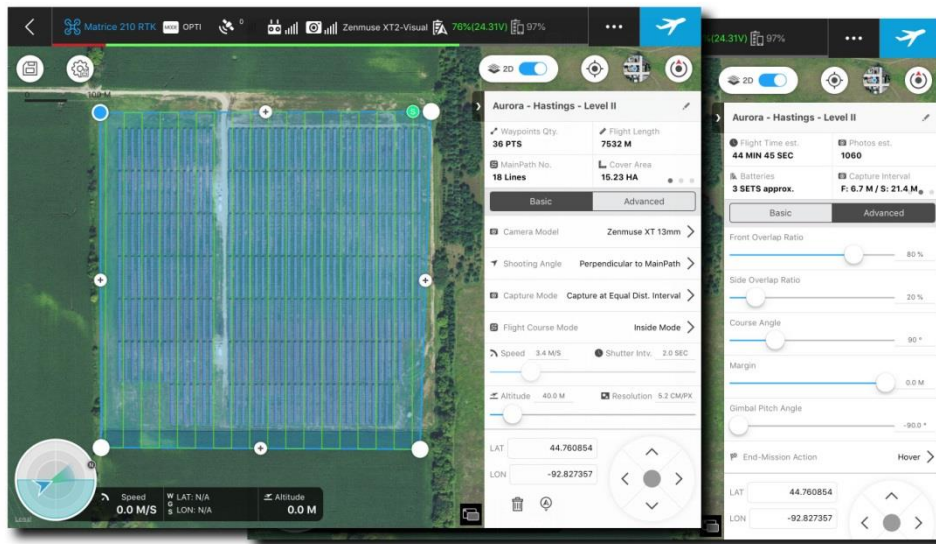


Figure 5.8 Sensor orientation

- Image metadata: set to capture GPS location, relative altitude, gimbal attitude, timestamp;

- Camera heading: constant UAS camera heading maintained if using multi-copter i.e. If UAS camera is facing North at start of inspection, it should remain facing North during entire inspection despite UAS' orientation;
- Image storage: high speed memory card with a UHS-3 rating (SanDisk Extreme suggested).



*Figure 5.9 DJI Ground Station Pro Settings for Level II flight*

Concerning high-resolution RGB (Red Green Blue) images, they can be used to verify and further classify anomalies that are identified in the thermal images. RGB imagery is also valuable to be used for an as-built basemap layer in the final report to aid in localization.

RGB images must respect the following parameters:

- File format: .jpeg;
- Gimbal pitch: straight down with deviation by up to 10° acceptable to avoid glare off the solar panels. Alternatively, sites with trackers the angle of the rows can be adjusted to avoid glare;
- Camera ground sample distance (GSD):
  - Flight altitude will depend on lens and desired GSD
  - 3.0 ± 0.5 cm/pixel is suitable for Level III inspections
  - 5.5 ± 0.5 cm/pixel is suitable for Level II inspections

- $15.0 \pm 5.0$  cm/pixel is suitable for basemap imagery
- Front & Side lap:
  - For Level II & Level III inspection the same front and side lap parameters should be as the thermal sensor. Typically, 80% front lap & 20% side lap.
  - For basemap imagery, 70% front lap & 70% side lap is required to generate an orthomosaic.
- Image metadata: set to capture GPS location, relative altitude, gimbal attitude, timestamp;
- Mission type: mapping mission with auto-capture.

Additional site images for reporting give a better idea of the inspected plant: oblique angle radiometric thermal images taken from high altitude and showing large sections of the site. These are helpful to quickly identify major faults and for executive summary reports.

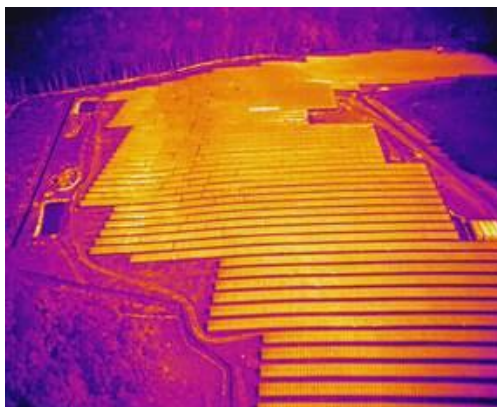


*Figure 5.10 Example of oblique image of PV plant*

After the flight, the last cautions:

- On-site quality-control check of the entire data set: confirm captured imagery of the entire site and data was captured in the correct format;
- Re-fly section(s) of the site that are missing data.

#### 5.5.4 Additional documentation

Other information will improve quality of final deliverables:

- as-built drawings, site documents, electrical diagrams (including site details such as module technology, wiring information, localization nomenclature/site numbering convention);
- Flight record (pilot, equipment, weather).

#### 5.5.5 Inspection time and delivery guidance

It is recommended to fly maintaining a range of similar high irradiance values, so the inspection should be conducted late morning through early afternoon.

A report delivery time of three days is required from the day of delivery of the data collected during the inspection.

A unified access to every EGP plants report is required, through a unique global profile, in which the plants are divided for Country.

# 6 Faults found in the field

## 6.1 Thermographic reports

Being only at the beginning of robotization process, some tests have been performed with different companies, among which there is Raptor Maps that, at the end, has been chosen since it has been considered the best in terms of quality and cost.

Enel Green Power operators with pilot’s license, using drone and camera belonging to the Country of reference, have made surveys.

The following reports come from different plants localised in North and South America: these are the result only of thermography because only an IR camera was on field. Hence, not having a double camera, visual inspection is not included. Another useful information concerning these PV plants is about their “age”, all of them are very “young”, since they have started the energy production for one year.

### 6.1.1 Plant 1: Rubi

This plant is localised in Peru, the following geographical coordinates: latitude (north) -17.253°, longitude (east) -71.189°. It is composed by 179,5 installed MW, but only 4 MW, and consequently 12500 modules, have been inspected. Following the result:

Findings					
Defect	Number	Est. Affected DC (kW)	Est. Affected DC (%)	Est. Impact per Hour (\$/hr.)	Est. Impact per Year (\$/yr.)
Cell	25	0.32	0.3	0.00	0.00
Diode	3	0.32	0.3	0.00	0.00
String	11	105.6	99.4	0.51	1275.00
total	39	106.24	100	0.51	1275.00

Figure 6.1 Rubi findings

### 6.1.2 Plant 2: Villanueva

This is the biggest Enel Green Power solar plant, in fact it boasts the capacity of 845,9 MW installed. It is situated in Mexico, at 25.596° of latitude (north) and -103.04° of longitude (east). Here half of the field has been inspected giving the following results:

	Tracker Anomaly	Motor Anomaly	String Outage	Module Failure	Diode Bypass	Hotspots
Villanueva I	243	119	315	27	912	104
Villanueva III	207	52	238	19	148	68
Villanueva EX	54	53	15	3	88	71
Total Issues	504	224	568	49	1148	243
Total Power Affected (MWdc)	14.515	6.451	5.453	0.016	0.121	0.001
% of Site Production Affected	1.716%	0.763%	0.645%	0.002%	0.014%	0.000%

*Figure 6.2 Villanuena findings*

### 6.1.3 Plant 3: Dodge Center

This solar plant and the remaining ones analysed in this thesis are in USA, they belong to one single project, a solar park composed by more fields smaller than the ones discussed above. They are close, Dodge Center has these coordinates: 45.452° of latitude (north) and -71.52° of longitude (east).

In this case, the entire field has been surveyed since it counts “only” 9.9 installed MW.

<i>Inspection Service</i>	<i>Inspection Coverage</i>	<i>Results</i>	
<b>General Site Overview</b>	Visual Imaging & orthomosaic creation of entire site, as well as general site summary	No cases of compromised Infrastructure were Identified.	
<b>Malfunctioning Module Identification</b>	Thermal Inspection of all panels	<b>Module Damage</b>	
		<b>Partial</b>	<b>Full</b>
		12	282
<b>Vegetation Growth Sampling</b>	Visual Inspection of key sample areas	Not requested.	
<b>Site Shading Analysis</b>	Topological modeling of entire site	Not requested.	
<b>Thermal Inverter Analysis</b>	Thermal Inspection of all inverters	Not requested.	
<b>Tracker Misalignment Review</b>	Visual Inspection of site	Not requested.	

*Figure 6.3 Dodge Center findings*

#### 6.1.4 Plant 4: Woods Hill

Woods Hill, included into Aurora, is located at 41.74° of latitude (north) and - 71.52° of longitude (east). Also this one has been inspected totally, in two tranches, east part and west part.

Findings					
Defect	Number	Est. Affected DC (kW)	Est. Affected DC (%)	Est. Impact per Hour (\$/hr.)	Est. Impact per Year (\$/yr.)
Cell	26	2.82	1.28	NaN	NaN
Multi Cell	3	0.49	0.22	NaN	NaN
Diode	5	0.54	0.25	NaN	NaN
Row	1	111.15	50.57	NaN	NaN
Soiling	455	73.94	33.64	NaN	NaN
String	5	30.88	14.05	NaN	NaN
Total	495	219.81	100	NaN	NaN

*Figure 6.4 East Woods Hill findings*

Findings					
Defect	Number	Est. Affected DC (kW)	Est. Affected DC (%)	Est. Impact per Hour (\$/hr.)	Est. Impact per Year (\$/yr.)
Cell	3	0.32	0.01	NaN	NaN
Multi Cell	1	0.16	0.01	NaN	NaN
Diode	4	0.43	0.02	NaN	NaN
Inverter	32	2432.95	97.87	NaN	NaN
Module	3	0.97	0.04	NaN	NaN
Soiling	10	1.63	0.07	NaN	NaN
String	8	49.4	1.99	NaN	NaN
<b>Total</b>	<b>61</b>	<b>2485.87</b>	<b>100</b>	<b>NaN</b>	<b>NaN</b>

Figure 6.5 West Woods Hill findings

### 6.1.5 Plant 5: Atwater

Atwater is a solar PV plant situated at latitude equal to 45.15° (north) and at longitude equal to -94.77° (east). Here 18000 modules are installed, corresponding to a capacity of 5.85 MW: the whole camp has been overlooked.

Findings					
Defect	Number	Est. Affected DC (kW)	Est. Affected DC (%)	Est. Impact per Hour (\$/hr.)	Est. Impact per Year (\$/yr.)
Cell	46	4.83	29.87	0.29	435.00
Multi Cell	16	2.52	15.59	0.15	225.00
Diode	12	1.26	7.79	0.08	120.00
Module	6	1.89	11.69	0.11	165.00
Tracker	1	5.67	35.07	0.34	510.00
<b>Total</b>	<b>81</b>	<b>16.17</b>	<b>100</b>	<b>0.97</b>	<b>1455.00</b>

Figure 6.6 Atwater findings

### 6.1.6 Plant 6: Paynesville

The last plant of this list is Paynesville, also part of Aurora. Localised at 45.39° of latitude (north) and -94.72° of longitude (east), it contains 46890 modules, namely 15,24 installed MW. The whole plant has been analysed.

Findings					
Defect	Number	Est. Affected DC (kW)	Est. Affected DC (%)	Est. Impact per Hour (\$/hr.)	Est. Impact per Year (\$/yr.)
Cell	945	99.22	36.32	5.95	8925.00
Cell Multi	136	21.42	7.84	1.29	1935.00
Diode	49	5.14	1.88	0.31	465.00
String	11	62.37	22.83	3.74	5610.00
Tracker	15	85.05	31.13	5.10	7650.00
total	1156	273.2	100	16.39	24585.00

Figure 6.7 Paynesville findings

## 6.2 Failures categorization

The whole study is based on the data detectable from these reports, it was tried to be as generic as possible, using average values to resolve the climatic differences due to the different locations of the plants.

The aim of this study is to understand the benefits that the use of drones instead of man, brings to the company. For this reason only the faults concerning the module have been considered, those ones about trackers or inverters have not been included because they cause a loss production big enough to be detected by other means of monitoring, i. e. power-irradiance curves. These controls have a frequency of once a month, so drones, used twice a year, do not have an impact on these errors detection.

At this point, it has been possible to understand which are the most common faults and their impact on module performance. Following the table that resumes all the failures found into the various reports.

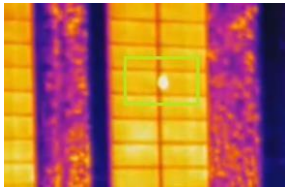
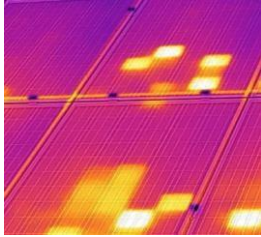
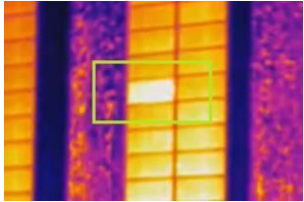
<b>Plant</b>	<b>Rubi</b>	<b>Villanueva</b>	<b>Dodge Center</b>	<b>Woods Hill</b>	<b>Atwater</b>	<b>Paynesville</b>
<b>Inspected MW</b>	4	391.6	9.9	24.45	5.85	15.24
<b>Inspected Modules</b>	12500	1223750	31428	75620	18000	46890
<b>Cell (#)</b>	25	243		29	46	945
<b>Cell (%)</b>	0.2	0.02		0.04	0.26	2.02
<b>Multicell (#)</b>			12	4	16	136
<b>Multicell (%)</b>			0.04	0.01	0.09	0.29
<b>Module (#)</b>		49	282	3	6	
<b>Module (%)</b>		0.00	0.9	0.0	0.03	
<b>String (#)</b>	11	568		13		11
<b>Modules in string (#)</b>	330	17040		247		198
<b>Modules in string (%)</b>	2.64	1.39		0.33		0.42
<b>Row (#)</b>				1		
<b>Modules in row (#)</b>				342		
<b>Modules in row (%)</b>				0.45		
<b>Bypass diode (#)</b>	3	1148		9	12	49
<b>Bypass diode (%)</b>	0.02	0.09		0.01	0.07	0.1

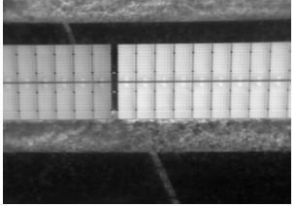
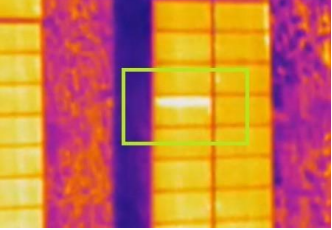
<b>Soiling (#)</b>				465		
<b>Soiling (%)</b>				0.61		
<b>Damaged modules (#)</b>	358	18431	294	1099	80	1328
<b>Damaged modules (%)</b>	2.86	1.50	0.93	1.45	0.44	2.83

*Table 6.1 Resume of thermographic reports*

From the data collected by inspecting more than 1000 MW, an average value of damaged modules has been calculated: 1.67%.

A brief description of anomalies is listed below:

Anomaly	Description
	Cell hot spot: beyond a hot spot there may be different causes, it is necessary to better investigate and the module is usually substituted
	Multi-cell hot spot: Multi-cell anomalies are indicated by multiple hot spots on the surface of the module. The majority of these anomalies are coincident with 'Fogged Modules', which typically indicates broken glass. The module must be replaced.
	Module: the entire module is open circuited, not connected to the system, as a result of handling, installation, or manufacturing issues.

	<p>String: fault in thirty contiguous modules due to possible failure of fuse or damage to cables</p>
	<p>Bypass diode: one third of the module is colder. The interested zone is shaded or soiled, and the bypass diode activates to avoid remarkable loss production</p>

*Table 6.2 Description of anomalies*

Basing on the causes and the relative correcting acts, a division of the failure in three categories has been done:

1. Cell and multi-cell represent thermal anomalies on the module, the last consequence is its substitution in field (orange category). Beyond these there can be many failures (see chapter 4.2.2) mainly based on the module's years of activity: in the first years PID, electrical mismatches, defects in the junction box and brown marks due to welding errors are more frequent. Over the years, however, the phenomenon of browning and corrosion of the surface of the module is more common. In the phase we are examining, therefore, the first ones are more present, but having to analyse the entire life of the plant, it has been decided not to subdivide the "hot spot" section into subcategories, giving an energy loss value of about 45% (orange category);
2. Module, string and row indicate a complete off-line, so they lead to a loss production of 100%. In this case, the source is basically electrical, in the sense that there is no damage to the modules themselves, but more damage to wires or protective equipment, i.e. fuses. The name of this category is "protection issues" and the colour of reference is green;
3. Activated bypass diode and soiling: the activation of bypass diode is a consequence of soiling or shading, so both these faults are pluggable to 1/3 of loss production and to a cleaning operation (blue category).

## MODULES FAULTS

■ module thermal anomalies ■ protection system issues ■ activated bypass diode

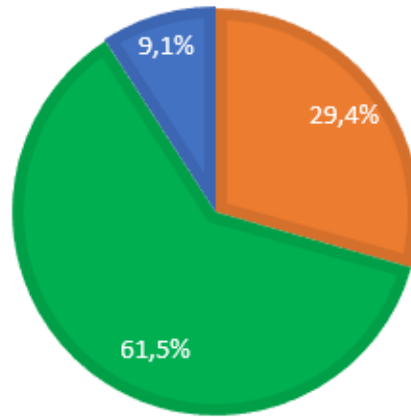


*Figure 6.8 Percentage of individual error categories*

The graph represents the frequency of the three different categories, in more than half of all cases the problem is due to connections or protective equipment: this is a good news considering that this category causes 100% energy loss but it is cheap to repair (it does not require module substitution), consequently there is ample scope for energy recovery

	Thermal anomalies	Activated bypass diode	Connections issues
<b>Frequency</b>	29.4%	9,1%	61.5%
<b>Energy loss</b>	45,00%	33,33%	100,00%

*Table 6.3 Energy losses associated to fault category*

## 6.3 Energy assessment

To understand the amount of energy loss associated to these failures, it is necessary to know the productivity of the plant, in terms of equivalent operating hours (EOH=kWh/kW per year).

The used model is based on hourly information of a whole year about solar irradiance ( $\text{W}/\text{m}^2$ ) and temperature ( $^{\circ}\text{C}$ ): these data are detected on PVGIS site by inserting field geographical coordinates, installed MW and tracker information (in the analysed plants trackers are always at single axis). This site returns a cvs file with a list of values of ambient temperature and irradiance relative to every hour of one year, considering weather conditions from 2005 to 2015. The irradiance is divided in beam, diffused and reflected, so the sum of these contributions gives the total irradiance to insert in the reference model.

At this point, the model calculates:

- Working T of the panel:  $T_c = T_{amb} + 30 * G/800$  (where G is irradiance);
- Power DC varying with irradiance:  $P_{DC}(G) = P_n * G/1000$  (where  $P_n$  refers to installed MW);
- Over or under temperature compared to  $25^{\circ}\text{C}$ :  $\eta_T = 1 - 0.005 * (T_c - 25)$  (where  $\gamma = -0.005$  and varies with technology);
- Production ratio:  $PR = \eta_T * 0.92 * 0.95$  (where 0.92 is due to optical losses on DC side and 0.95 is the efficiency of the inverter);
- Power on AC side:  $P_{AC} = P_{DC}(G) * PR$ .

Once calculated these hourly values, reference yield and PR are used to find our interest value: the final yield, i.e. equivalent operating hours  $Y_f = Y_r * PR$ .

Actually, this datum is available in the description of the plant given by Enel Green Power, so a comparison has been made.

<b>Plant</b>	<b>EOH using theoretical model</b>	<b>EOH given by EGP</b>
<b>Rubi</b>	2304	2259
<b>Villanueva</b>	2683	2720
<b>Dodge Center</b>	1367	1387
<b>Woods Hill</b>	1400	1418
<b>Atwater</b>	1418	1437
<b>Paynesville</b>	1433	1450

*Table 6.4 Equivalent operating hours for each PV plant*

The differences are minimal, EGP values have been taken into account for the study, and an average has been done obtaining the value 1778 MWh/MW. The aim of this study is to understand how much only modules failures contribute to energy loss, so starting from average EOH and considering an energy availability of 97.5% the gross production is 1824 MWh/MW.

$$energy\ availability = \frac{produced\ energy}{produced\ energy + energy\ loss}$$

Hence, if into the whole plant there are no losses a module produces 0.58 MWh per year (0.0015 MWh per day).

## 6.4 Energy losses

The information needed to define energy losses associated to module failures in the whole life of a plant is the panels failure rate, the frequency of the different causes and the relative energy loss.

The last two have already been made known (table 6.3), while the first point has been the most difficult to determine: the available data are about plant one year old, so it has not been easy to understand how the failure rate evolves in time. The only possible solution has been to approximate the trend of failure rate to the bathtub curve.

The bathtub curve qualitatively represents the failure rate trend during the physical life of a complex system. Three singular areas of the curve are identified: the area of early failure (or infant mortality, where the failure rate is decreasing with time and is due to manufacturing or installation errors), the area of physical life (where the failure rate remains constant with respect to time), and the area of generalized wear (or wear out, where the failure rate becomes very rapidly increasing). Knowledge of this scheme, even if of a qualitative nature, is of fundamental importance in the economic evaluation of maintenance policies.

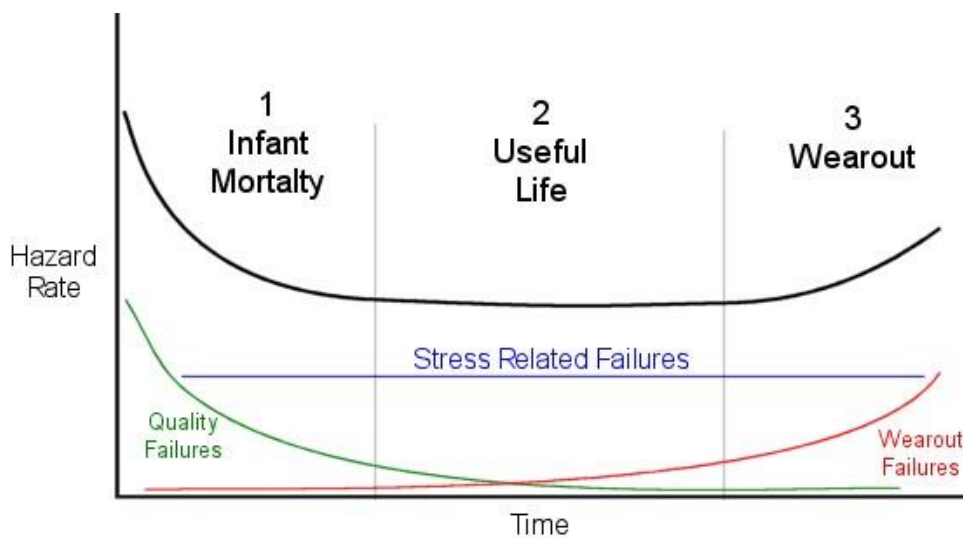


*Figure 6.9 Bathtub curve*

To give a quantitative value to this graph many hypotheses have been made:

- Infant phase: it goes from the first to the fifth year and at the end of this period the failure rate touches its minimum values, 0.5%;
- Middle phase: it lasts eleven years and the percentage of damaged module is constantly 0.5;
- Old phase: this last period lasts eight years and the failure rates increase again until a value of 1.14%

These values do not derive from empirical study, but from suppositions and approximations made with EGP engineers who have been working in photovoltaic sector for many years.

In this way, it has been possible to obtain values for every year and to draw two exponential lines and one straight-line obtaining the following graph:

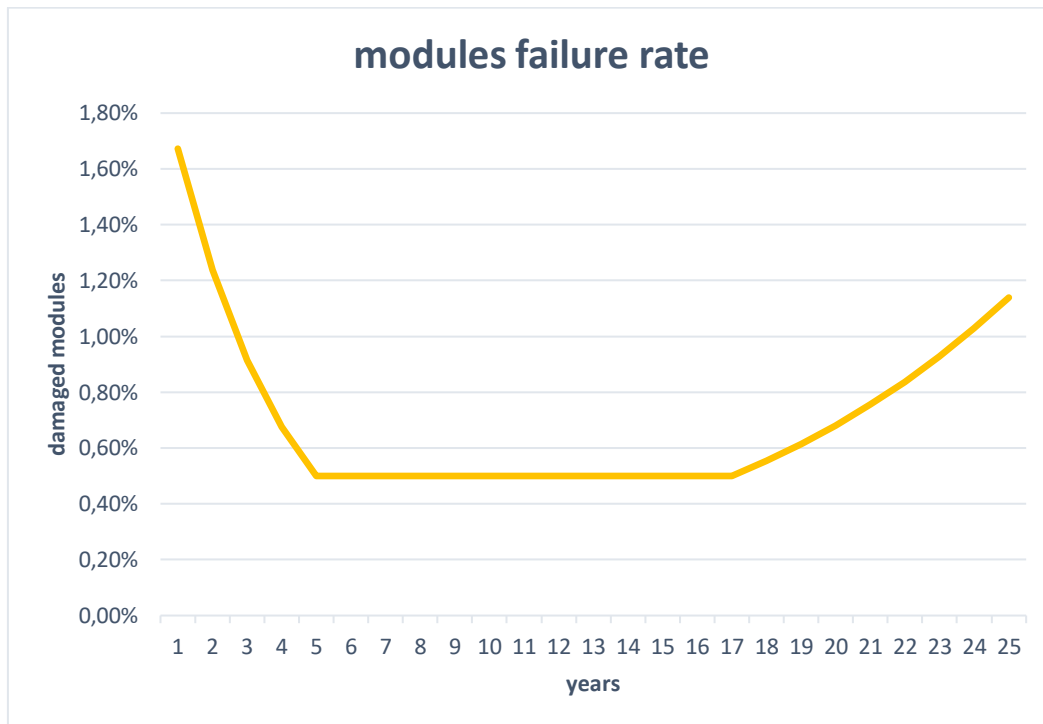


*Figure 6.10 Module failure rate in 25 years*

At this point, an economic model has been created: it analyses cost and benefits derived from the use of drones and it is established in such a way that, inserted the size of the plant (installed MW), it returns the cumulative cash flow curve.

# 7 Economic Analysis

## 7.1 Net Present Value methodology

Among the various techniques for evaluating investments, the one considered as the main reference is the Net Present Value methodology. The basic idea is to compare the returns of a specific investment project with the opportunity cost of the capital used to finance the project.

The methodology consists in calculation of net gain/loss on investment by discounting at time  $t_0$  of all incoming and outgoing cash flows, using an adequate discount rate. Cash flow is a measure of the company's self-financing, the objective of which is to define the cash generation of a company and consequently the attribution of these cash flows to its shareholders.

The cash flow can be calculated starting from the changes in the balance sheet balances between two reference periods, but in practice, the company's income statement is also used to help determine the items that constitute it. For example, instead of disclosing changes in balances between different periods of an amortisation fund (a liability account on the balance sheet) it is often easier and more immediate to disclose the value of the amortisation (a cost on the income statement).

The flow takes into account the numerical changes (income and expenditure) that may occur:

- Inbound, we speak then of cash inflow;
- Outbound, we speak then of cash outflow.

Hence, for a new project, the net present value can be calculated as follows:

$$NPV = -C_0 + \frac{C_1}{(1+r)} + \frac{C_2}{(1+r)^2} + \frac{C_3}{(1+r)^3} + \dots$$

$$NPV = \sum_{t=0}^{t=n} \frac{C_t}{(1+r)^t}$$

Where they are:

t: time limits;

C<sub>t</sub>: financial flow (positive or negative) at time t;

r: interest rate at which the transaction is carried out.

The decision rule is: if NPV > 0 the project can be realised, otherwise rejected.

Usually the rate (r) coinciding with the Weighted Average Cost of Capital (WACC) is used.

It represents the average cost of capital that the company pays to all its investors, shareholders and creditors and it is defined by the following formula:

$$WACC = \frac{E}{K} * y + \frac{D}{K} * b * (1 - t_c)$$

Following the table with meanings of symbols

symbol	meaning	unit
c	weighted average cost of capital	%
y	required or expected rate of return on equity (cost of equity)	%
b	required or expected rate of return on debt capital (cost of debt)	%
t <sub>c</sub>	tax rate	%
D	total debts	currency
E	total market value of equity capital	currency
K	total capital invested in the company (D + E)	currency

*Table 7.1 Component for WACC calculation*

NPV methodology is flanked by several alternative techniques, including the most common payback period.

The term payback period refers to the period of time needed to recover funds spent on an investment, thus reaching the break-even point. In the following formula n is the payback period.

$$\sum_{t=0}^{t=n} \frac{C_t}{(1+r)^t} = 0$$

## 7.2 Application

Net Present Value methodology has been implemented during this study; in particular, it has been useful to understand, in terms of plant size, when it convenes to buy a drone and to pass from manual thermography to automatized one.

The first step has been the division of the costs in capex and opex. Capex derives from capital expenditure, it is the cost of developing or providing durable assets for the product or system. Opex, from the English term operating expense, is the cost necessary to manage a product, a business or a system (otherwise called Operation and Maintenance costs or operating and management costs).

### 7.2.1 Capex

In our case capex are the ones concerning drone and batteries purchase cost, camera price and the expenditure of training Enel Green Power operators to become drone pilots.

CAPEX	€/drone (DJI M600 Pro) # drone/100 MW	5.699,00 € 1	5.699,00 €
	€/extra batteries # extra batteries/drone	1.254,00 € 3	3.762,00 €
	€/camera (Zemuse XT2 640x512, 13o19mm) # camera/drone	9.990,00 € 1	9.990,00 €
	€ training/person people/drone	5.000,00 € 2	10.000,00 €
	<b>TOT CAPEX</b>		<b>29.451,00 €</b>

*Table 7.2 Capex*

Considering that, regardless of installed MW, EGP buys only one drone, this capex is fixed. All the other items in fact, depend only on drones number: three extra batteries per drone, two operators per drone and one camera per drone. Hence, the investment cost of this project is € 29.451,00.

## 7.2.2 Opex

Totally different is the opex, it varies with size plant, so with installed MW. The items are four:

1. Maintenance hardware cost: precautionary sum to deal with possible damage on the various hardware. This item is fixed;
2. Drone change: it has been considered the purchase of a new drone every five years. Also this is constant;
3. Cost per survey: cost for analysing images, hence Raptor Maps price;
4. Maintenance plant cost: the principle cost regards field maintenance, hence modules substitution, electrical damage repair, hence the corrective actions for the three categories of errors seen in chapter 5.

In this list the most variable points are the last two, let us dwell on these.

It has already been analysed Raptor Maps pricelist, for the first inspection of a level 2 quality, the cost is 56 €/MW. For the succeeding surveys, the company offers some discounts: 5% for the second inspection, 10% for the third one, and 20% from the fourth onward. This point is obviously variable with plant size.

The maintenance plant cost instead, has two different variables: field size and percentage of defected modules, so it varies during the years too. For the three categories of faults seen before, there are three different corrective actions and the relative costs.

When the error is a thermal anomaly on the module, the consequence is the replacement of the module: in the first ten years of operation the warranty covers the entire panel cost, only the labour and the decommissioning costs have been considered, equal to 30 €/module (20 + 10). After the expiry of the assurance, also the panel price has been taken into account. To estimate what the cost of a module in ten years will be it has been accounted the New Energy Outlook, the economic analysis made by Bloomberg New Energy Finance.

As detectable from the following graph, the cost is continuously descending and in this analysis a price of 0.13 €/W has been set, reaching a value of 41.6 €/module,

so in the second part of plant life a total price of 71.6 €/module for the whole corrective action is considered.

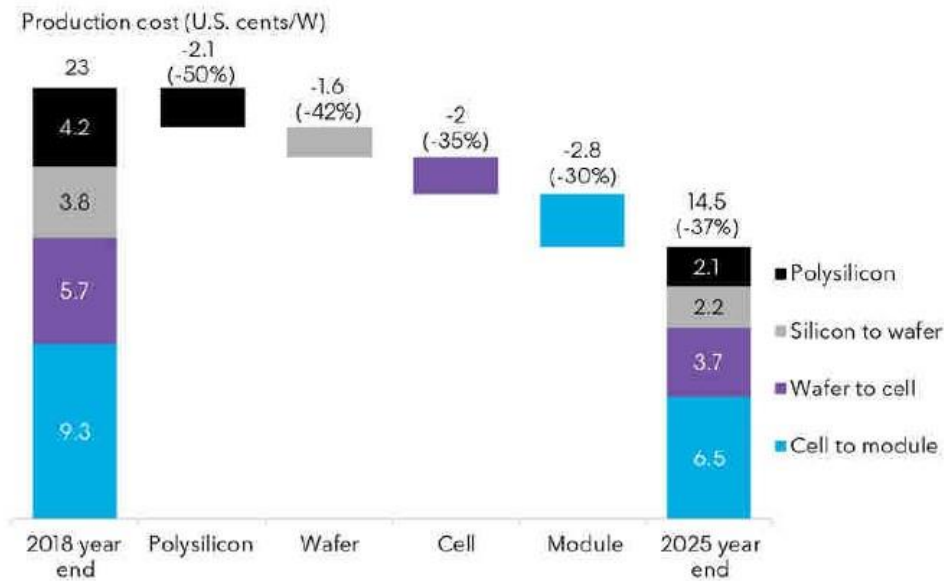


Figure 7.1 Forecasts on module price

For the fault category “activated bypass diode” the most common cause is dirt, consequently the corrective action is just cleaning, so the cost in this case has been set equal to 0 €/module, since it’s negligible.

Finally for what concerns connections issues, the entity of the fail is variable, hence it has been considered the cost of intervention in the field of the team, equal to 30 €/hour. In this study this value is imposed like 10 €/module, in fact it often happens that with an intervention issues of more modules are solved.

Once established these three maintenance costs, basing on every category frequency, the definition of this opex item is concluded.

### 7.2.3 Incomes

At this point, the economic benefits of the use of drones are investigated, they are principally two: savings passing from manual survey to automatized one and income due to recovered energy. Let us see them in more detail.

The transition from manual to drone inspection obviously leads to great time savings, just think that manually it is possible to inspect 2.3 MW/day, while with drone 24 MW/day.

The first value has been set considering that the thermography can last 4 hours/day to have a good irradiance and that man speed is 2 seconds/module. The second value is extracted from operators experience in field, to fly over 8 MW one hour is necessary, time including battery change; furthermore every day it must be considered one additional hour for setting up, take-off and landing.

This difference of time equates to a big opex saving that grows in a directly proportional way with plant size and also to hours on added value activities, it means saved hours for best and faster activities: the delta of time between the two methodology can be recovered and made useful for other activities.

For what concerns recovered energy, the number of surveys per year principally causes the difference: manually it is just one/year, while with drone two per years have been established. The following hypothesis has been done: in case of manual inspection, the faults can persist in field averagely six months, with the passage to drones it reduces to three months. At this another value must be added, the difference of time between the two surveys is time in which energy is recovered, too. The consequent income is due to those 90 days (six months minus three months) plus the delta variable with plant size, days during which modules work and produce energy. This item changes both with installed MW and with time, since it depends on failure rate, too.

As already specified, these values are function of size and amount of damaged modules, to give an idea of how much it is possible to earn, let us consider a plant of 100 MW at its fifth year of activity, when the failure rate has already decreased and equal to 0.5%. The delta cost/survey is roughly equal to € 69.000, the energy recovered is about 271 MWh, and setting the cost of energy at 50 €/MWh, the gain during this year is 13550 €.

## 7.3 Conclusions

Once examined capex, opex and incomes, the cash flow is evaluable: following a summarising table.

CAPEX	OPEX	INCOMES
<ul style="list-style-type: none"> <li>• Drone</li> <li>• Additional batteries</li> <li>• Camera</li> <li>• Training</li> </ul>	<ul style="list-style-type: none"> <li>• Survey</li> <li>• Drone maintenance</li> <li>• Maintenance of the plant</li> <li>• New drone every 5 years</li> </ul>	<ul style="list-style-type: none"> <li>• Savings compared to manual method</li> <li>• Recovered MWh</li> </ul>

*Table 7.3 Costs and incomes*

Photovoltaic plants lifetime is estimated at 25 years, hence the Net Present Value at 25 years has been calculated, changing only the size: this allow recognising in which plants a drone should be bought and where it is better to continue with manual methodology, or to share the hardware with other fields.

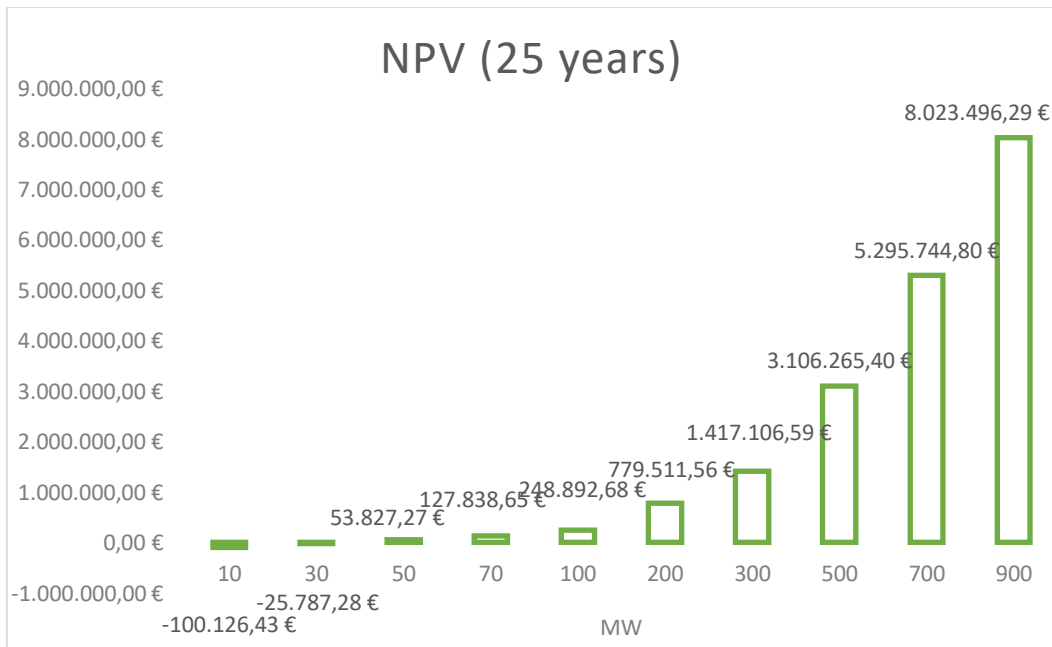


*Figure 7.2 NPV at 25 years for plants with different size*

As detectable from the graph above, the convenience increases with plant size. It is the expected result, obviously the larger the field the greater the gain due to delta costs in comparison with traditional means, the bigger the amount of recovered energy, too.

Following two examples of graphs representing 30, 50 and 500 installed MW: there is a huge difference. In the first case, incomes are so lower than costs that the fixed expenditure for new hardware every five years contributes a lot in curve variation. In the 50 installed MW plant, the investment begins to be convenient, the new hardware cost is still visible. In a big plant instead, it is does not stand out looking at the graph, since it is a small contribution compared to the sums involved.

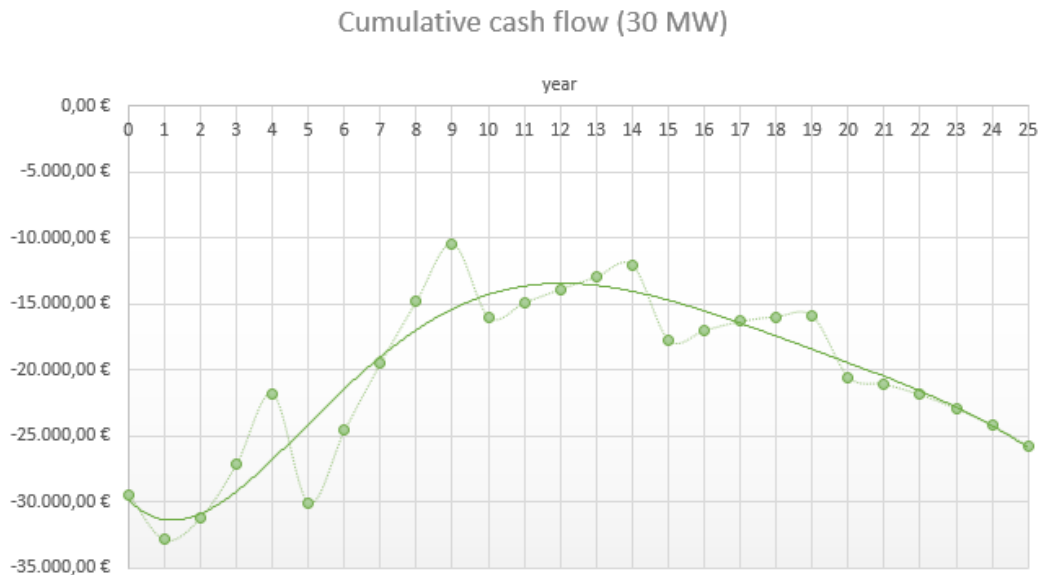


*Figure 7.3 Cumulative cash flow for 30 MW plant*

Cumulative cash flow (50 MW)

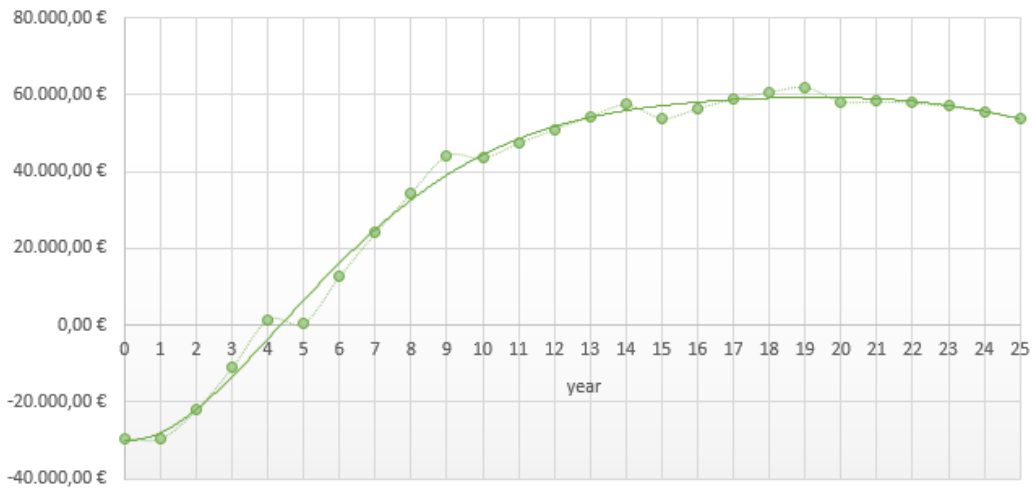


Figure 7.4 Cumulative cash flow for 50 MW plant

Cumulative cash flow (500 MW)

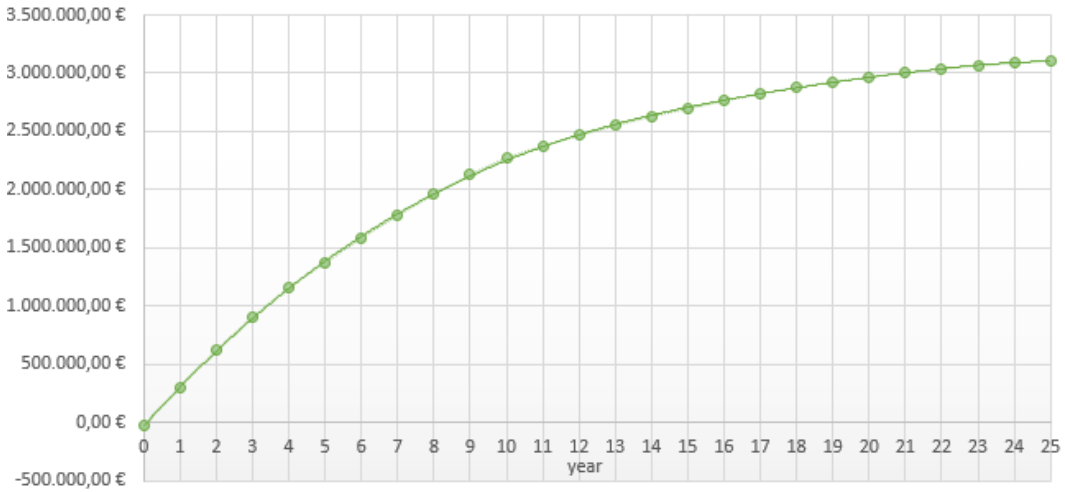


Figure 7.5 Cumulative cash flow for 500 MW plant

In addition, the payback time has been calculated, the table with the results confirms what has just been said.

<b>Installed MW</b>	<b>PBT [years]</b>
10	never
30	never
50	4,629
100	1,887
200	0,564
300	0,252
500	0,071
700	0,0177
800	0,0038

*Table 7.4 Pay Back Time*

In the end, it convenes to implement UAS when the installed MW at least 50, under this value it is better to continue with manual surveys or, if distances allow it, to share one drone among little plants.

## 8 Future evolutions

Nowadays drones are the ready-to-market technology: they are cheap, reliable and easy to drive. They have some limitations anyway, they always need a pilot, someone to drive them and change the battery when it runs out, and so they require a person to be present in field.

The challenge for the future is to go beyond these limits and make operations as autonomous as possible. From this perspective, Percepto was born: the Percepto Core™ relies on real-time machine vision and advanced AI technology to bring to life a fully autonomous drone that performs multiple security, safety and inspections without the need for human intervention.

This kind of intelligent drone can fly without human control, it simply follows a path inserted in its memory and it can be set off from remote; it is also able to recharge itself thanks to its platform, the real strong point of this technology.



*Figure 8.1 Photo of the first Percepto flight in Totana, Spain*

Hence, it is possible to activate, deactivate and even destroy it (through a special self-destruction button) remotely: in this way, it becomes an autonomous instrument whose use is not limited to thermography. It can be used for surveillance, in fact when someone crosses the perimeter of the field, it raises the alarm and flies to the point of violation filming the intruder.

The most interesting use of this autonomous drone is surely data capture: when the company manages to have its own software for the analysis of RGB and IR images, once a week or once a day, the drone can fly and take pictures. Images collected at short time intervals are useful to understand how the plant degrades basing on climate, years of operation, technology implemented.

Data and artificial intelligence are the technological combination of the moment, and in this way, they are used in maintenance too, particularly in predictive one. The management of the plant would become really easier.

The immediate reception of the error present in the field by the head office would facilitate the communications and would greatly simplify the work.

At this time, it is still in the testing phase and Enel Green Power does not have its own software for images analysis, and the cost of Percepto is too high to be bought by every Country, so it must weight some years to see this technology in every EGP plant.



## **Bibliography**

Photovoltaic/Thermal (PV/T) systems: Status and future prospects - Ali H.A. Al-Waelia, K. Sopiana, Hussein A. Kazemb, Miqdam T. Chaichanc - Renewable and Sustainable Energy Reviews(2017), pp. 1-3

Renewables 2018 - Global Status Report (GSR): Ren 21, pp. 90-100

Photovoltaics and wind status in the European Union after the Paris Agreement-Roberto Lacal Arantegui, Arnulf Jäger-Waldau - Renewable and Sustainable Energy Reviews (2017), pp 2460–2471

Review of Failures of Photovoltaic Modules - International Energy Agency, pp 61-85

Introducing electroluminescence technique in the quality control of large PV plants – Jorge Coello, pp 2-5

Research on hot spot risk for high-efficiency solar module – S. Deng, Z. Zhang, C.Ju, J. Dong, Z. Xia, X. Yan, T Xu, G. Xing, pp 78-82

New Energy Outlook 2018 – Bloomberg NEF, pp 29-30

Analisi delle performance giornaliere e di lungo termine di sistemi fotovoltaici e caratterizzazione delle perdite termiche - B. Herteleer, pp 79-83

Impact of energy losses due to failures on photovoltaic plant energy balance – I. Lillo-Bravo, P. González-Martínez, M. Larrañeta, J. Guasumba-Codena, pp 2-4

The crucial role of materials in protecting the longevity of solar investments – DuPont Photovoltaic Solutions, pp 7-12

Assessment of Photovoltaic Module Failures in the Field - International Energy Agency, pp 28-53

Utilizing unmanned aircraft systems as a solar photovoltaics operations and maintenance tool – Electric Power Research Institute, pp 4-7

Power generation - pantries prof. F.Spertino

Internal documentation- Enel Green Power

## Ringraziamenti

Questo è uno dei giorni più importanti della vita, il traguardo che per molto tempo sembra irraggiungibile, il momento atteso con ansia, ma che si vive con un briciolo di malinconia. In questo giorno non posso fare a meno di ringraziare chi ha reso possibile tutto ciò.

In primo luogo grazie al professor Filippo Spertino, sempre gentile e disponibile. Prima come professore e poi come relatore è stato di grande ispirazione, i suoi consigli sono stati per me fondamentali.

Questo lavoro di tesi non esisterebbe senza Vincenzo e tutto il Solar Competence Center di Enel Green Power, grazie per questa fantastica prima esperienza lavorativa e per avermi calorosamente accolta, sin da subito.

Un doveroso ringraziamento va alla mia numerosa famiglia, in primis a mamma e papà, tutto quello che ho realizzato sino ad oggi lo devo a voi, grazie per la fiducia e il sostegno costanti. Grazie alle mie sorelle e alle mie bellissime nipotine, portatrici di gioia sempre. Un ringraziamento speciale a Marisa e Giuseppe, che mi hanno supportata in questi ultimi mesi e con i quali ho condiviso il momento più bello della loro vita, è stato un onore.

Grazie a Paolo, sempre presente e soprattutto paziente: mi hai aiutato a superare le avversità di questi anni sopportando i miei innumerevoli sbalzi d'umore. Averti accanto nella mia vita è solo la prima tra le tante cose per cui esserti grata, non farò un elenco infinito qui, semplicemente grazie.

Ringrazio i miei amici, i vecchi, quelli che sono purtroppo lontani, ma che nonostante ciò non mancano di far sentire il loro affetto. Tra tutti grazie a Margherita, il tempo e la distanza non fanno altro che rendere questo rapporto sempre più forte, la nostra amicizia è uno dei pilastri portanti della mia vita.

Alla mia nuova famiglia torinese, a tutti coloro che ho conosciuto in questi due anni e che hanno riempito giornate e serate rendendole indimenticabili. Grazie Federica per essere stata il mio primo punto di riferimento in questa città, le lunghe e profonde chiacchierate con te sono sempre piacevoli. Grazie Elisa per le risate e i memes, per i momenti divertenti vissuti insieme. Grazie Giacomo, coinquilino e amico, la mia vita a Torino non sarebbe stata la stessa senza di te, grazie per il continuo pessimismo e la poca voglia di vivere, grazie per le serate in casa e non, e grazie per la bella persona che sei. Grazie Antonio, Benny, Anna e

tutti coloro che, anche solo per un momento, mi hanno fatta sentire a casa nonostante questa fosse a 1000 km di distanza.

Dal biliardino di casetta a quello del Tabacchi, dal Poliba al Polito, dal mare alle montagne, grazie ai miei inseparabili colleghi per la compagnia e il sostegno costante nei momenti di intenso studio.

Infine grazie anche a me stessa, per non aver mollato e per averci creduto sempre, anche quando sembrava impossibile. E' finita!

Torino, 26 Marzo 2019